AN ABSTRACT OF THE THESIS OF

William Clyde Russell for the M.S. in Civil Engineering (Structures)
(Name) (Degree) (Major)

Date thesis is presented May 3, 1966

Title EXPERIMENTAL STUDIES OF VIERENDEEL BEAM ANALYSIS

Abstract approved Redacted for Privacy
(Major professor)

Fabricated steel beam specimens with rectangular holes cut in the webs were subjected to load tests to analyze the behavior of the modified section. Beam-depth to hole-depth ratio was in all cases 2.0; however, ratio of hole length to hole height varied from 2.0 to 3.0. The primary instrumentation of electrical resistance strain gages was located at ratios of nominal bending moment to shear for the solid section of 40 and 64. Instrumentation was located with regard to flexural behavior in the tee-sections, rather than the determination of stress concentrations near the hole corners.

The approximate Vierendeel method, although not new, is developed for the analysis of beams with web holes; such beams are commonly called Vierendeel beams. Also included is a more precise development of the Vierendeel analogy by matrix analysis techniques. Experimental strain results are correlated with predictions by both the approximate Vierendeel analysis, which is currently used for design analysis, and by the actual Vierendeel analysis. Experimental deflection results are correlated with deflection predictions by the

actual Vierendeel analysis. Predictions by the theory of elasticity method are discussed, but due to the complexities of the solution, comparisons with the experimental results are not presented.

Tests in which the beam specimens were loaded to failure were conducted to study the type of failure when web material is removed. Failure was a form of lateral instability before the desired failure mode was obtained.

EXPERIMENTAL STUDIES OF VIERENDEEL BEAM ANALYSIS

by

WILLIAM CLYDE RUSSELL

A THESIS

submitted to

OREGON STATE UNIVERSITY

in partial fulfillment of
the requirements for the
degree of

MASTER OF SCIENCE

June 1966

APPROVED:

Redacted for Privacy

Professor and Head of Department of
Civil Engineering

In Charge of Major

Redacted for Privacy

Dean of Graduate School

Date thesis is presented May 3, 1966

Typed by Muriel Davis

ACKNOWLEDGMENTS

This thesis project is by a sole author; however, numerous contributions have been made, without which, this end result may not have been possible. Cooper & Rose and Associates, engineering consultants, have contributed financially, along with their many ideas, to the continuation of the web-hole studies. Fought and Company fabricated the beam specimens used in this particular project. With an award fellowship to the writer, the American Institute of Steel Construction has sponsored this investigation. Encouragement, technical assistance, and invaluable instruction were received from Professor Thomas J. McClellan and Dr. Harold I. Laursen. Joseph Grant, graduate student, contributed immensely by his sincere interest and continued encouragement. Due to her genuine attempt to understand and contribute throughout the course of this project, from initial data-recording to final proof-reading, the writer's wife was largely responsible for this end result.

The writer wishes to extend his sincere gratitude and thanks to these individuals and companies who have lead to the completion of this thesis project.

TABLE OF CONTENTS

LIST OF FIGURES

LIST OF FIGURES (continued)

LIST OF TABLES

NOMENCLATURE

A	Cross-sectional area of the member.
b^i	Connection width at the i end of the member
b^j	Connection width at the j end of the member
B^i	Ratio of the corrected connection width at the i end of the member to the free span of the member.
B^j	Ratio of the corrected connection width at the j end of the member to the free span of the member.
C^i	Empirical adjustment factor for a connection width at the i end of the member.
C^j	Empirical adjustment factor for a connection width at the j end of the member.
e	Axial deformation of the member.
E	Modulous of elasticity of the material - assumed 29,500,000 pounds per inch squared for A36 steel.
I_B	Moment of inertia of the solid beam about is neutral axis.
I_t	Moment of inertia of the tee-section about its neutral axis.
$[k]$	Matrix relating internal displacements to external displacements for the complete structure.
$[k_i]$	Matrix relating internal displacements to external displacements for the i^{th} member.
ℓ	Free span length between connections for the member.
L	Span length of the member from center to center of joints.
M	Bending moment at a point in the solid beam.
M^i	Bending moment at the i end of the member.
M^j	Bending moment at the j end of the member.

P	Axial force in the member
P_T	Total load on the test beam.
V	Shear force in the member.
x	Longitudinal distance on a tee-section from the hole center line to a particular point.
$[x]$	Correction constants to be applied to $[k_i]$ for connection width considerations for the member.
y	Transverse distance from the solid beam neutral axis to a particular point.
y_t	Transverse distance from the tee-section neutral axis to a particular point.
y_{tb}	Transverse distance from the tee-section neutral axis to the hole edge.
$\overline{y}$	Transverse distance from the tee-section neutral axis to the nearest outer flange.
η	Deflection at the i end minus the deflection at the j end.
ϕ^i	Rotation at the i end of the member.
ϕ^j	Rotation at the j end of the member.

EXPERIMENTAL STUDIES OF VIERENDEEL BEAM ANALYSIS

Part 1

INTRODUCTION

A design engineer usually designs a member for varying loads, but is not always required to consider any circumstances which might change the member's load carrying properties. At times, steel wide flange beams which had been placed in a building framework have had holes cut in the webs to allow placement of pipes and heating ducts. This reduces the floor-to-floor distance as the ducts and pipes do not have to be placed below the beams, and therefore also, reduces the total height of the building. The removal of the web material creates an entirely different member with respect to the stresses that are developed in the beam when compared to the solid-web member. Various engineers now design members (beams) which have holes in the web for building construction. The benefits derived from such design practice are threefold: (1) story-to-story distances reduced, (2) accessibility for plumbing placement, and (3) weight reduction of beams. A limitation of this practice is the uncertainty of the design methods since very little is known about the behavior of a beam with part of the web material removed.

Due to the uncertainty of the present design methods, more experimental work must be performed in test laboratories to justify the analysis presently being used and to develop easier, more accurate predictions of the behavior of such beams. This thesis project involves the testing of beam specimens and the correlating of results with analytical calculations.

Purpose of Study

Two beam specimens were obtained and instrumented with SR-4 electrical resistance strain gages. The beams were of similar proportions, except for the aspect ratios of the holes (the length of the hole along the axis of the beam divided by the height of the hole) which varied between specimens. A complete description of the test specimens is included in Part 2. The specimens were subjected to numerous load tests with varying load positions, thereby causing nominal bending moment to shear ratios at the hole center lines between ten and infinity. The principal instrumentation was at a hole which had moment to shear ratios of 40 to 64. In these initial or primary tests, the stresses calculated from the measured strains were limited to the elastic range of the material. The measured strains were to be compared with the strains calculated by the analytical procedures presented herein. The intent of these comparisons was the purpose of this study: to show that the behavior of the test specimens can be adequately predicted by analytical methods.

Prediction of the beam behavior applies to both the linear stresses and the deflections, but not to the stress concentrations at the hole corners.

After completion of the primary tests, the beams were loaded to failure in the ultimate load tests. It was anticipated that the failure of the beam would occur in the region of the web hole. Such a failure would contribute to the development of yield theories due to the stress concentrations, and also to the development of an ultimate-strength design method (3, p. 13). Although such a failure did not occur, the actual failure did contribute to this study.

Review of Previous Research

Previous research in this area, although limited, has been developing rapidly in recent years. The American Institute of Steel Construction recently sponsored an investigation (16, p. 4) of reinforcement requirements around web holes. In that research report the author introduces a theoretical approach based on the assumption that the beam acts as a Vierendeel truss in the area of the hole, if this hole is centered on the neutral axis. Presentation of the method, as used in previous literature, is shown in Part 4 of this thesis in conjunction with the experimental comparisons. The Vierendeel truss approach is similar to the slotted beam analysis presented by Roark (12, p. 45). In Part 5 a more precise use of the Vierendeel truss analogy is developed, presented, and compared with experimental determinations.

Experimental work in the area of the Vierendeel truss can be traced to the work of Professor Arthur Vierendeel, who in 1897 designed a simple rigid truss without diagonals for a bridge to be load-tested (1, vol. 107, p. 1215). This type truss, sometimes called a "ladder" truss or an "arcade" truss, became known as a Vierendeel truss, due to the extensive work by Professor Vierendeel on this type truss. Experimental work on the "beam-type" Vierendeel truss has been limited to very recent years.

Experimental results (13, p. 5) have also been correlated with analytical calculations using the terms "moment-bending" (bending of the solid beam) and "shear-bending" (bending of the tees above and below a web hole caused by cantilever action). This method yields the same calculated stresses as the Vierendeel analysis since the method in either case amounts to the same procedure. To the writer's knowledge, this experimental work by Roik and Almdal (13) is the only report in which the experimental deflections are reported.

Other experimental work has been performed at McGill University and correlated with theoretical calculations by the theory of elasticity. This work at McGill University is reported in the McGill University Applied Mechanics Series and briefly described by Bower

(4, p. 5). The beam specimens used in these tests were rolled shapes with holes 16 inches long and beam depth to hole depth ratio of 1.75. These beam specimens had the longest holes of any previously tested and reported upon (to the writer's knowledge).

The Applied Research Laboratory of the United States Steel Corporation has recently completed an extensive investigation and development of the application of the theory of elasticity to the web hole problem (2, p. 1). In a subsequent report (3, p. 5) experimental results are compared to the analytical calculations by both the theory of elasticity and the Vierendeel analysis. Octahedral shear stresses are emphasized in these reports.

Previous studies (9) sponsored by the Oregon State University Engineering Experiment Station have been performed on a prefabricated beam specimen, and the experimental results related to those of the Vierendeel analysis. This thesis project is a continuation of this previous work.

Part 2

EXPERIMENTAL PROCEDURES

Test Specimens

Beam specimens were fabricated of ASTM A36 steel throughout. Two 1/2 inch by 4 inch rolled flange plates were welded to a 1/4 inch by 14 inch web plate, thus forming a "I" beam cross-section 15 inches in height. Two beams of such cross-section were fabricated, each 12 feet long, weighing approximately 25.5 pounds per foot. Web holes were then torch-cut in the web plates in the arrangement as shown in Figure 1. As shown, all holes were rectangular in shape, and had 1 inch radii rounded corners. The holes were left in the as-cut condition, and no allowances were made in the experimental calculations for any case-hardening effects in the material adjacent to the hole. Both beams are symetrical about the neutral axis (holes centered on the neutral axis), and also about the center line of the beam. The depth of beam to depth of hole ratio (depth ratio) is in all cases 2.0 and the aspect ratio was either 2.0 or 3.0. Emphasis is placed on the aspect ratio; the largest previous aspect ratio was 2.0.

Inspection of Figure 1 indicates a narrow web plate between the edge of the hole and the end of the beam. It was concluded after reviewing previous studies (5, p. 34) that no web buckling would occur

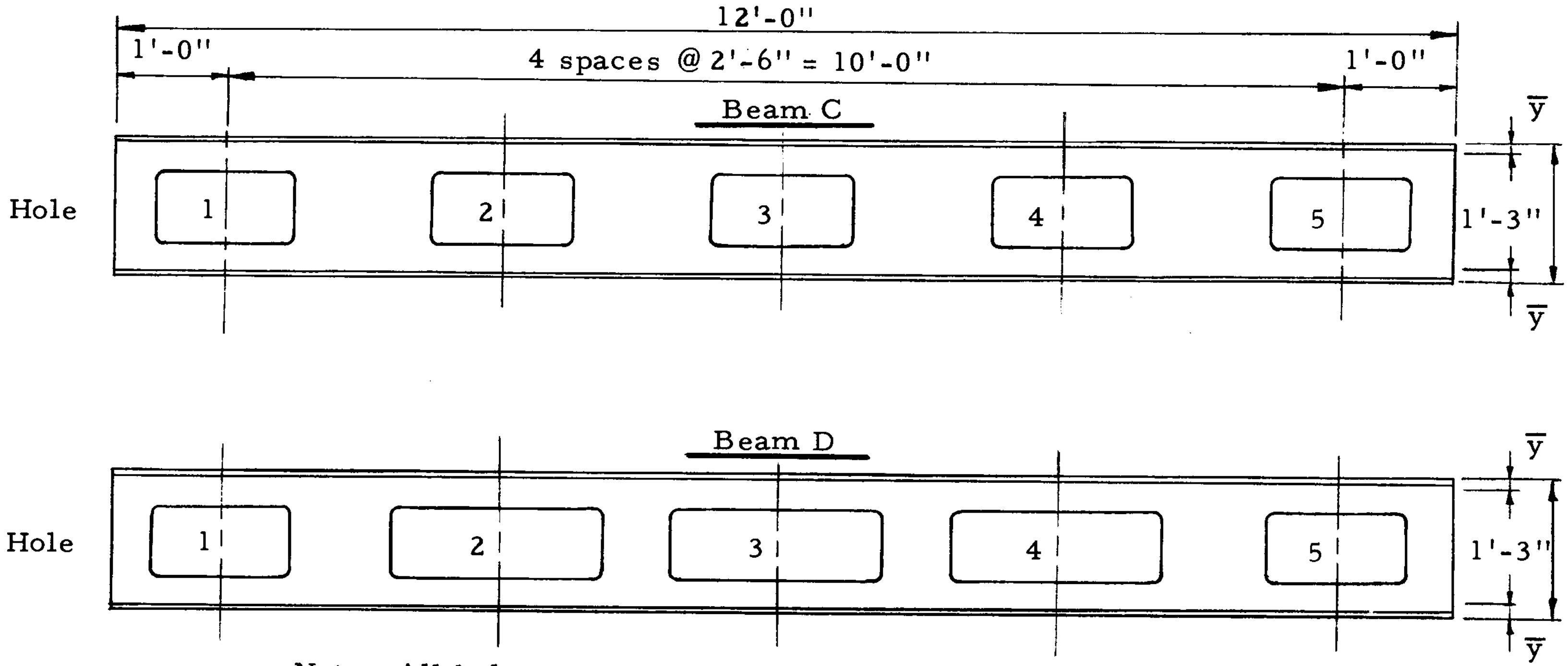

Note: All hole corners rounded to 1 inch radius.
Scale: 1 inch = 20 inches

Beam	Hole lengths, in.					Hole Depth in.	I_B, in.^{4}	I_t, in.^{4}	$\bar{y}$, in.
	1	2	3	4	5				
C	15.0	15.0	15.0	15.0	15.0	7.5	269.5	2.79	0.81
D	15.0	22.5	22.5	22.5	15.0	7.5	269.5	2.79	0.81

Figure 1. Test specimens.

in this web plate. Due to the welding of the flange plates to the web plate, a slight amount of plate curvature could be detected in both the tension and the compression flange of the beam. This curvature is shown, greatly exaggerated, in Figure 2. The vertical deflection of the edge of the flange plate was approximately 1/32 of an inch. No adjustments were made in the calculations, but this curvature would affect both the bending behavior of the beam and the residual stresses in the flange plates.

Figure 2. Flange Curvature

Instrumentation

Each beam was instrumented with electrical-resistance strain gages, as shown in Figure 3, and a photograph of the arrangement is shown in Figure 4. Linear gages were type A-7 gages with 1/4 inch gage lengths, and the rosettes were the rectangular type with 1 inch gage lengths. All gage lead wire was 18 gauge wire size. Terminal boards were used for connection of the lead wires from the gages to

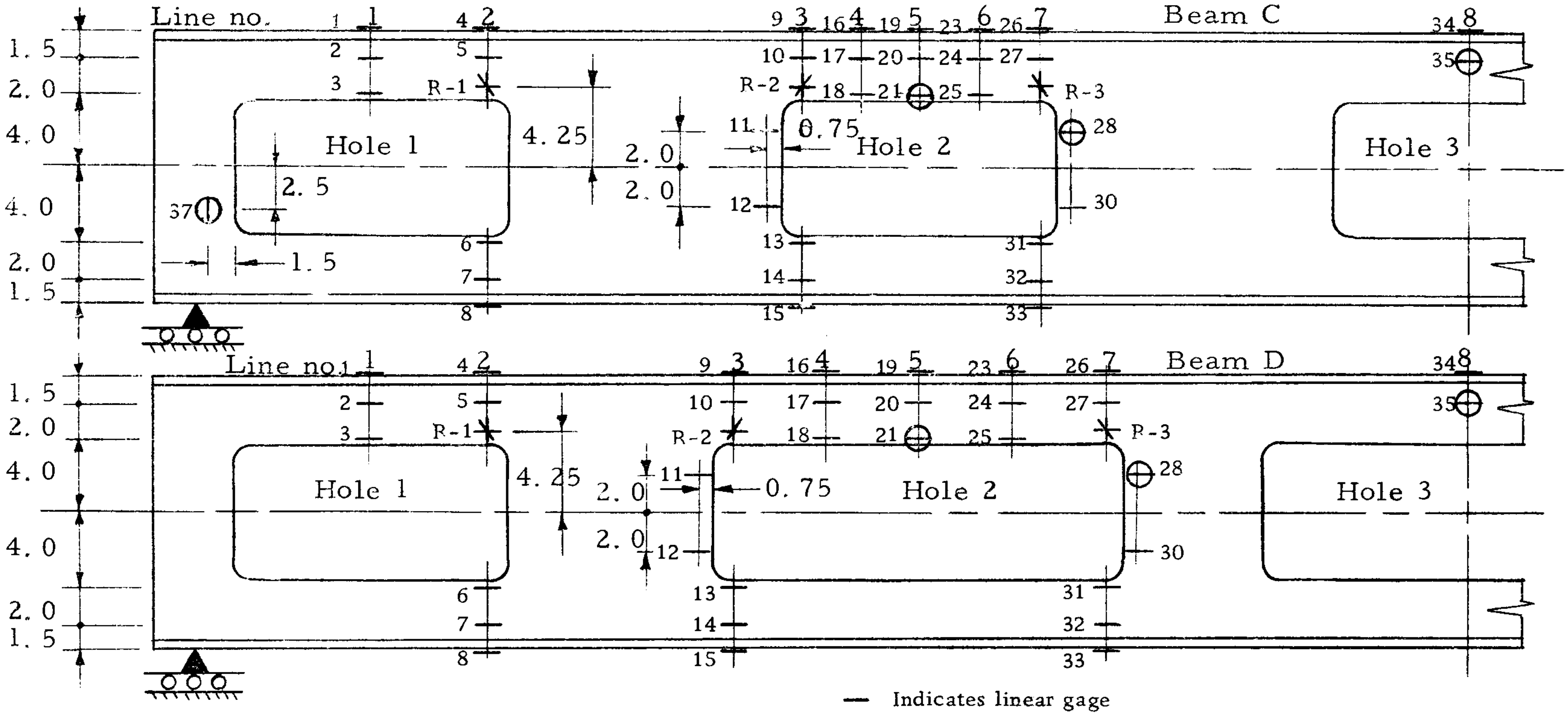

NOTE: Dimensions are in inches

Scale: 1 inch = 10 inches

LONGITUDINAL DISTANCE FROM LEFT REACTION, INCHES								
Beam	Transverse line of gages no.							
	1	2	3	4	5	6	7	8
C	9.50	16.00	33.00	36.25	39.50	42.75	46.00	69.50
D	9.50	16.00	29.25	34.37	39.50	44.62	49.75	69.50

Figure 3. Gage locations shown schematically with the small type being indicative of the gage numbers.

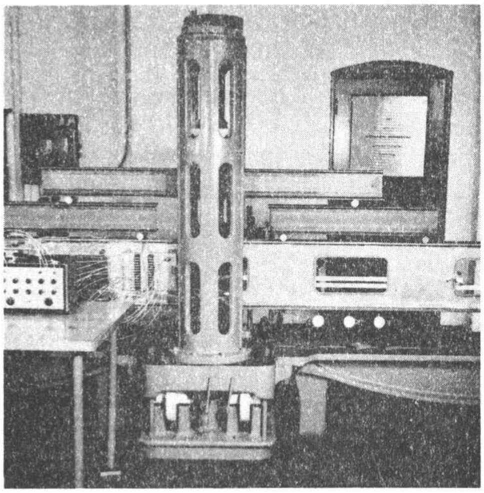

a) Beam C under load type 1.

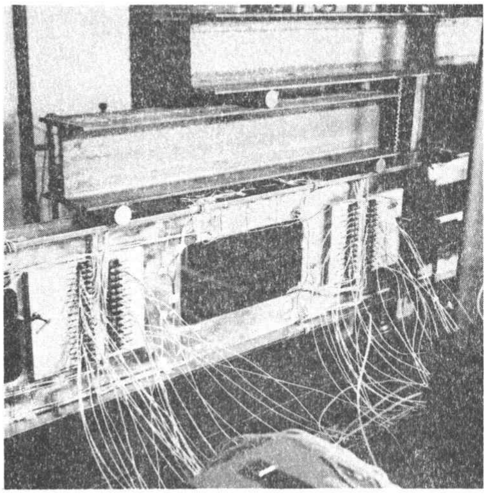

b) Beam C close-up.

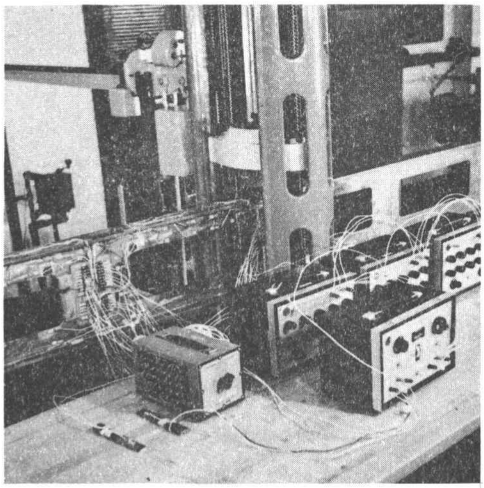

c) Beam D under load type 2.

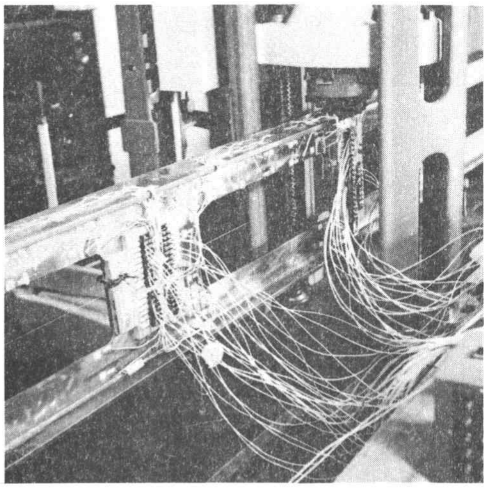

d) Beam D close-up.

Figure 4. General photographs.

the lead wires on the switching units, as shown in Figure 4.

A Baldwin Strain Indicator, Model 20, with digital read-out was used for strain readings. Figure 4 shows the test setup with the strain indicator and switching units shown.

Deflection measurements were taken by two different methods. A small brass wire was stretched between the neutral axis, directly above one support, to the corresponding position at the opposite end of the beam. With a telescope located approximately 10 feet from the side of the beam, deflection measurements were read from metal scales taped to the web of the beam at 2 different locations. The second method of observing deflections was by the placement of Ames dials beneath the lower flange. The Ames dials can be seen in Figure 4. Agreement between the wire deflections and the dial deflections was very poor. However, since internal reference was used with the wire method and external reference used for the Ames dials, the deflections measured by the wire method are considered more accurate. Therefore, all reported deflections in this thesis are those measured by the wire method.

Placement of the strain gages was based partially on previous research, and partially on the particular effect being sought. The main emphasis was not on the stress concentrations near the hole corners, as Lander's investigation (9) deals primarily with instrumentation at the hole corners. The Applied Research Laboratory

(3, p. 9) also dealt primarily with the stress concentrations near the corners. It is of interest, however, to note that the stress concentrations are reduced if larger radii hole corners are used (14, p. 53). Verification can also be shown experimentally by studying results of circular web holes (an extreme radii of corners equal to 1/2 the hole length), as shown in Bower's experimental work (3, p. 6).

However, in the determination of strain gage locations, emphasis was on linear strains in the tee-section above Hole 2. The heavy instrumentation of this tee-section was to determine the actual behavior of this area. The beam-column action of this tee was to be studied under the assumption that this tee-section may be designed as a beam-column.

Test Procedure

All load tests were performed in a 150, 000 pound Rhiele mechanical testing machine. Each beam was tested under three different types of load arrangements. These load arrangements are shown schematically in Figure 5, and photographs are shown in Figure 4. For type 1 load arrangement, the load distributing members were of 6 x 6 WF 15. 5 sections with a total weight of approximately 180 pounds. To approximate concentrated point loads, 1-1/2 inch steel rollers were used for type 1 loading.

Before load tests were begun, the beam was preloaded, or

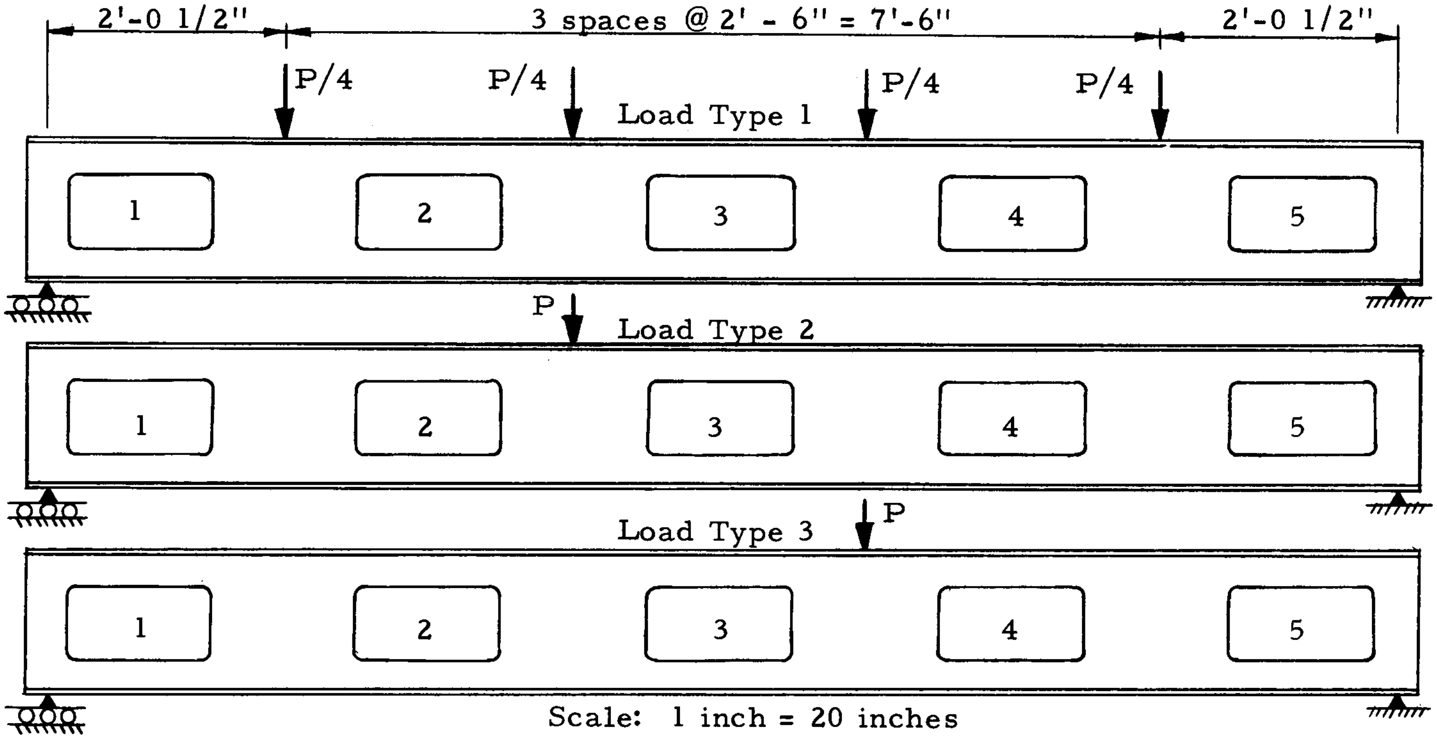

Load Type	Max. P_T, kips		Nominal Moment to Shear Ratio				
	Beam C	Beam D	Hole 1	Hole 2	Hole 3	Hole 4	Hole 5
1	14.0	12.0	10	64	∞	64	10
2	10.0	8.0	10	40	70	40	10
3	10.0	8.0	10	40	70	40	10

Figure 5. Beam C in load schematics (Beam D similar).

preflexed, to a predetermined stress level, such that the strain gage readings would stabilize. The initial tests (called the primary tests) were conducted such that measured strains were limited to within the elastic range of the steel. After initial strain readings were taken, the total load in each case was increased in increments of 2,000 pounds, with all strain readings taken after each load increment. Three load tests of each of the load types were conducted in an attempt to obtain good average readings (due to the similarity of type 2 and type 3, only one load test was performed for load type 3). All strain readings shown herein are weighted averages of three load tests.

After all elastic load tests were completed, a failure test (called the ultimate test) was performed using load type 1 arrangement. All previous tests were loaded at a rate of approximately 5,000 pounds per minute; however during the ultimate load test the loading rate was reduced by about one-half.

Part 3

ANALYSIS OF TEST DATA

In order that the analytical methods to be presented in Parts 4 and 5 can be clearly related through the development of the analytical equations to the experimental results, the test results are presented and discussed before the discussion of the analytical procedures.

Primary Load Tests

To simplify the presentation of the experimental results, all strain data has been plotted for easy comparison and placed in the Appendix. Analytical curves are shown in conjunction with the experimental results, such that the points of failure and/or high accuracy of the analytical calculations can be easily seen. Deflection data is tabulated as recorded by the wire method (see Part 2), and compared to the theoretical calculations of Part 5.

Deflection Analysis

Experimentally determined deflections are tabulated in Table 1. If deflections were to be calculated manually, using a reduced moment of inertia where the web material is removed and applied in the moment-area method, calculated deflections would be approximately

1/2 the experimental results. Failure of this method is due to the large proportion of the bending that occurs in the area of the hole.

Table 1. Center Line Deflections (inches) By Wire Method

Beam	Load Type	Experimental	Connections Not Included	Connection Widths Reduced
C	1	0.120	0.194	0.108
	2	0.115	0.220	0.123
	3	0.110	0.223	0.090
D	1	0.125	0.173	0.112
	2	0.120	0.181	0.123
	3	0.090	0.168	0.091

However, beam deflections are often a limitation in building design. As can be seen in Table 1, the deflections calculated by the actual Vierendeel analysis are very conservative when the members are considered from center line to center line of the joints, but are accurate for instances where the connection widths are included and reduced as described in Part 5. Further discussion of the applicability of this method of deflection analysis is presented after the development of the method.

Strain Analysis

The experimental strains are presented in the Appendix in two different methods. In Figures A.1 through A.8 the experimental strains are plotted on transverse lines through a reduced beam section. Distribution of the strains are shown in the transverse direction by these figures. Figures A.9 through A.12 illustrate the distribution of the experimental strains longitudinally through the tee-section above Hole 2. These illustrations show the actual bending behavior of the tee-section above the hole. Experimental results are not presented for load type 3 due to the similarity of type 2 and type 3 results. Results shown for type 2 load tests are indicative of the type 3 load tests results.

In conjunction with the experimental strains, the theoretical strains are plotted on an identical basis as are the experimental values. As will be shown in Part 5, the results of the actual Vierendeel analysis were not the exact solution for the beam when loaded with the type 2 arrangement. Therefore, the actual analysis results are not plotted for the load type 2. As shown in the type 1 plots, both the actual Vierendeel and the approximate Vierendeel solutions yield linear predictions which are closely related.

Emphasis must again be placed on the type of results sought. The placement of the strain gages around the hole was not with the intention of determining the stress concentrations. Although the stress concentrations did affect some of the strain readings, no attempt will be made in the thesis to predict directions and magnitudes of the concentrations. The analysis briefly described in Part 6 could be used to predict the corner stress concentrations (3, p. 12).

In general the linearity of the strain measurements with increasing load was very good. However, at low strain levels, precise strain measurement was not possible due to the low strain itself. Nevertheless, these low strains are generally insignificant in the analysis.

Agreement between the theoretical strains and the experimental strains at the rosette gage R-3 (right-upper corner of Hole 2) is closer for beam C than for beam D. Disagreement at this point is caused by laws of continuity. The strains in the web plate between Holes 2 and 3 would be almost identical to the strains in a solid beam at this relatively high bending moment. Linking the high compressive strains caused by the "moment-bending" to the higher "shear-bending" tensile strains at the corner of the hole would cause a discontinuity at this corner. Thus, with the high stiffness of the web plate between the holes, as compared to the tee-sections, the strains caused by the "shear-bending" would be reduced to a level between the strain due to "moment-bending" and that caused by "shear-bending."

It may then be thought that the same type redistribution would occur at the same corner of Hole 1 (gage R-1). However, in this instance the moment-bending is relatively low. Thus, as might be expected, Figures A.5 and A.7 show that theoretical values are much closer to the experimental values at this location.

Other than the extremely stiff vertical web plate between the holes, which causes some strain redistribution in the tee-section, the test beams appear to behave as a Vierendeel truss. Near the center of the hole, it is indicated that excellent agreement is obtained. This is especially true of the agreement at an infinite moment to shear ratio (refer to Figure 5). The point of contraflexure, which is indicated in Figures A. 9 through A. 12 as the point of intersection of the 3 longitudinal lines of gage readings, appears to be in excellent agreement in all cases. This, of course, is indicative of the Vierendeel behavior of the beam. Note that the point of contraflexure is not at the center line of the hole, as generally assumed. This point of reverse bending will be discussed further when the approximate method of analysis is introduced.

Experimental rosette results at the maximum load for each load type are tabulated in Table A. 1. Methods used in the calculations are found in most strain analysis texts (11, p. 54). The horizontal stresses, which would generally be used for design, vary from the corresponding principal stresses between approximately 8 percent to greater than 40 percent error. The difference between the horizontal stress and the principal stress at the rosette R-3 (see Figure 3) is in every case greater than 25 percent. These large disagreements at R-3 are caused by the stress concentrations due to the high bending moment of the gross section. Note that since R-1 is in an area of constant bending moment to shear ratio, the disagreement between horizontal and principal stresses should be relatively constant for all load types. This is exactly the case; all disagreement is approximately 19 percent. The direction of the principal stresses at R-1 is also relatively constant for both beams, as might be expected.

Although the effect of the close spacing of the holes would be of interest, the geometry of the test beams complicates any such interpretations. Since Hole 1 is at the same location on each beam, the effect of the small width of remaining web plate between Hole 1 and Hole 2 should be reflected in the behavior of Hole 1. However, with a limitation of the instrumentation at Hole 1, the change in the behavior due to this closeness of Hole 2 could not be detected. Study of Figures A. 1, A. 3, A. 5, and A. 7 shows that in all cases the behavior of the hole is very similar. Thus it could be concluded that either the instrumentation provided was insufficient for such determination, or the small width of remaining web plate between the holes does not affect the behavior of Hole 1 under the conditions tested.

Ultimate Load Tests

With the completion of all primary tests, the ultimate test was performed on each beam in order that the type of failure could be

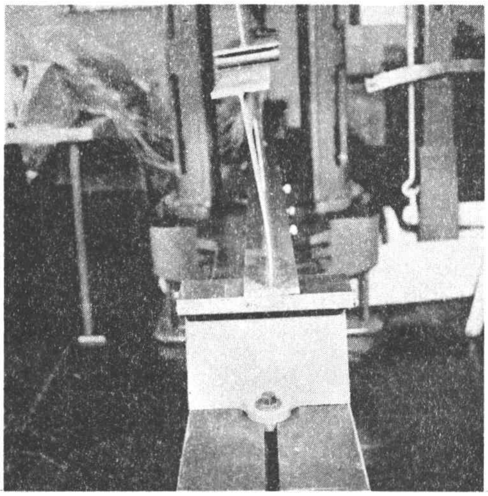

a) Beam D at failure.

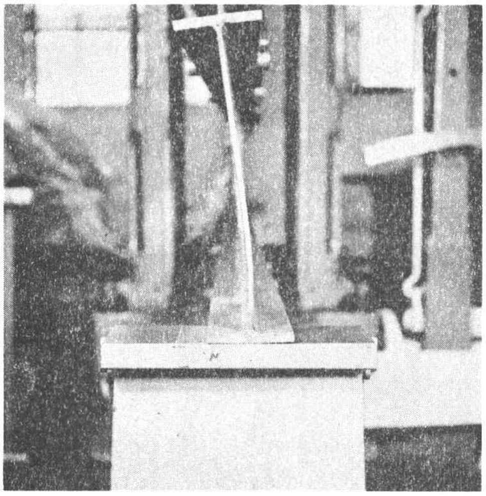

b) Beam D at failure.

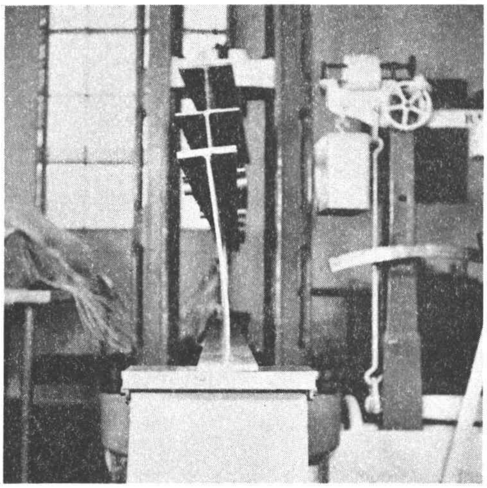

c) Beam D at failure.

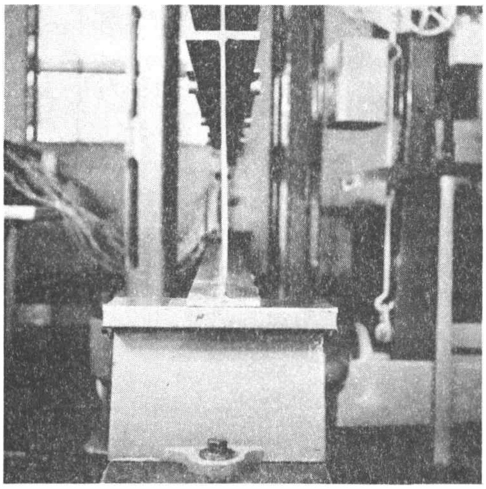

d) Beam D after failure.

Figure 6. Failure photographs.

studied. Beam D was failed first with a total load of 24, 000 pounds in the type 1 load arrangement. The failure was a form of lateral instability in the web near the ends of the beam. Photographs of the failure are shown in Figure 6. Strain and deflection readings had been taken at 22, 000 pounds with the observation that the strains at the critical corners were not stable. Just as the load was balanced at 24, 000 pounds, a sudden drop in the beam-arm occurred. The applied load was reduced to approximately 18, 000 pounds at which point the load remained steady.

Close inspection of the photographs would show that the upper flange has remained straight. The upper flange at one support of the beam deflected approximately 2-1/2 inches to one side, and this flange at the other support deflected approximately the same distance to the opposite side. To the writer's knowledge, the cause of such a failure could have been attributed only to the weakness of the web plates directly above the supports. Lateral load could have been introduced by tipping of the rollers on the rounded flange plates (see Figure 2), and thereby contributing to this failure. The failure of beam C was identical to that of beam D, except that the beam C failure was progressive. Bending in the web plate could be detected by close inspection at 12 kips. As shown by the photograph after failure, the failure was almost entirely elastic.

Curves illustrating the changes in the strains measured by the critical gages in the corners with changes in the total load are shown in Figure A. 13 for beam C and Figure A. 14 for beam D. All other gages were indicating regular linearity. The explanation of the behavior of gage R-1 between 12 and 16 kips in each beam can be stated in terms of the relatively high shear in this area. The stresses indicated by this gage are much higher than anticipated, considering only the solid beam bending. Thus, the stresses indicated are highly influenced by the high shear force. The non-linearity of gage R-1 must, therefore, be due to shear stress yielding in this region.

The highest strains indicated in the flange plates were located at the right edge of Hole 2, above and below the hole. In the case of beam D, these strains were approximately 700 micro-inches per inch at failure. Thus, although the beam was failed, no strains beyond the elastic limit of the material were recorded in the flange plates. Also of interest was the indication that even though high strains were being recorded near the hole corners, no instability of any kind was observed in the tee-sections at the holes upon beam failure.

Part 4

APPROXIMATE VIERENDEEL THEORETICAL SOLUTION

This method is based on an early presentation by Roark (12, p. 145) for analysis of slotted beams. Application of this method to steel beams with web holes is generally referred to as the approximate Vierendeel solution. Although various previous research reports (3, p. 18) and (15, p. 148) have presented the general method of approximate Vierendeel analysis, a brief presentation will be developed herein. However, since the method is very straightforward, it actually needs little more than a brief introduction.

Assumptions and Development

An accepted practice in the design of a Vierendeel truss was the assumption that points of contraflexure occur at the center of the vertical members. For the approximate Vierendeel beam analysis, however, somewhat different assumptions are made.

Consider a beam with a web hole in bending as shown in Figure 7.a. If the web hole is centered on the neutral axis of the beam, the assumption that the shear at the hole is equally divided between the upper and lower tee-sections will introduce little error. This is seen to be a reasonable assumption when considering the equal moment of inertia of both tee-sections. Equations by Roark (12, p. 145) split the total shear in proportion to the ratio of the moments of inertia in the two tee-sections.

To illustrate the second assumption which is made for analysis, consider the beam section as shown in Figure 7. b. Also consider that this reduced section is placed in pure shear, i. e., the bending is entirely in the tee-sections and no rotation takes place at the ends of the tee-sections. This, of course, will yield equal bending moments at the ends of each tee-section, and also, a point of contraflexure at the center of the span. Thus, the second assumption of this analysis is as follows: a point of contraflexure occurs at the center of the hole span, considering "shear-bending" only.

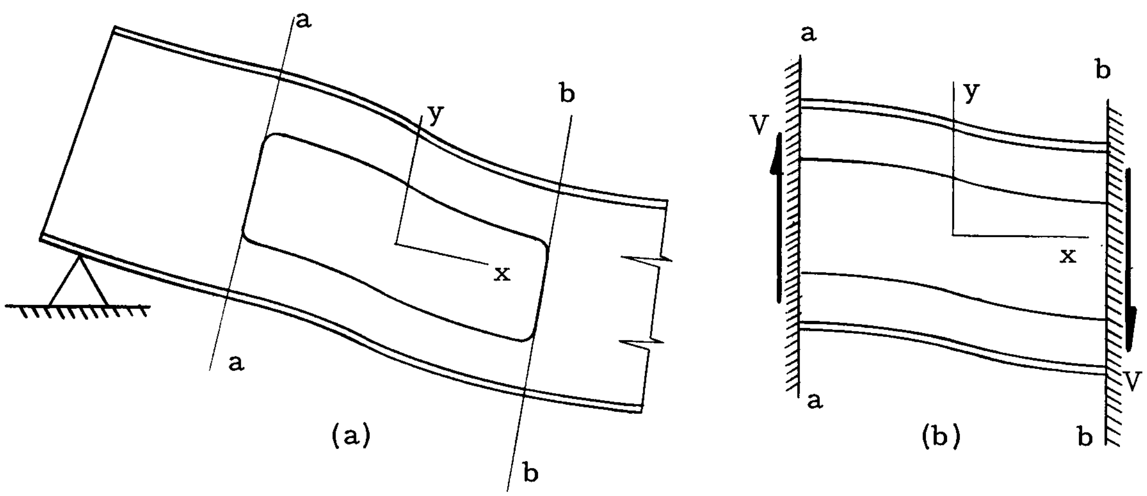

Figure 7. Beam sections. (a) actual section
(b) shear section

The stresses around the hole are then simply a summation of the two effects at the hole: (1) the gross-beam bending moment stresses calculated as for a solid beam, and (2) the tee-section "shear-bending" moment stresses calculated as for a cantilever using the previously described assumptions. Thus, the resulting equation for the total normal bending stress, σ is given by the equation:

$$\sigma = \frac{My}{I_B} - \frac{Vxy_t}{2I_t} \tag{1}$$

where for a particular point on one of the tee-sections:

M = bending moment of the solid beam,

y = distance from the solid beam neutral axis,

I_B = moment of inertia of the solid beam about its neutral axis,

V = total shear at the hole center line,

x = longitudinal distance from center of the hole,

y_t = distance from the tee-section neutral axis, and

I_t = moment of inertia of the tee-section about its neutral axis.

Note that the sign convention used is the same as that generally used by elementary mechanics of materials texts and that the x and y quantities are with reference to the coordinate system shown at the hole in Figure 7.b. Inspection of this equation shows that the combination of stresses are additive at the top of the upper tee-section and opposite at the bottom of this tee-section for the high moment side of the hole. The reverse is true at the low moment side of the hole.

Although unused in this thesis, the shear stress, τ, in the tee-sections can be given by the equation (3, p. 19):

$$\tau = \frac{V}{4I_t} \left(y_{tb}^2 - y_t^2 \right) \qquad (2)$$

where y_{tb} = distance from the tee-section neutral axis to the hole edge.

Due to the summation of the two terms in Equation 1, the actual point of inflection in the tee-section will always occur to the low moment side of the hole. This fact, although confusing when reviewing the initial assumption of center line contraflexure, can be justified by considering the change in slope of the solid beam between the two edges of the hole. A change in slope of the solid beam between the edges of the hole will occur when the beam moment is not constant over the length of the hole. This change in slope between the ends is reflected by a shifting of the moment diagram and also, of the resulting inflection point.

Application to Specimens

Theoretical calculations for this method are extremely simple and straight-forward. Equation 1 was used directly in the calculations in which only M and V are dependent on the varying load arrangements. Systematic calculations are easily arranged, by noticing the constant terms in each of the components of Equation 1 for a particular gage location.

Reference should again be made to Figures A. 1 through A. 12. As would be expected, the Vierendeel analysis always predicts linear strain distributions both longitudinally and transversely. Once again it is noted that excellent agreement between theoretical and experimental strains is obtained near the center of the hole.

Excellent agreement is also obtained between the theoretical point of contraflexure and the experimentally determined inflection point in the upper tee-section of Hole 2. However, since instrumentation was limited on the lower tee-section, no indication could be concluded as to the location of the inflection point in this tee-section.

Part 5

ACTUAL VIERENDEEL THEORETICAL SOLUTION

The approximate Vierendeel analysis makes use of two assumptions which can, in a more precise use of the Vierendeel analogy, be eliminated. This method, called the actual Vierendeel analysis in this context, would be very tedious, and hardly worthwhile since it is only an analogy, to perform by manual calculations. However, with the use of a high speed digital computer, the analysis becomes little more than routine. Although the results used herein were computed with the use of a digital computer, the same results would be obtained if a manual classical method was used. Such a comparison has previously been presented (16, p. 62), and therefore, no manual computations are deemed necessary.

Assumptions and Development

The principal assumption of this analysis is that a beam with numerous web holes actually behaves as a Vierendeel truss, and therefore, can be reduced to a "beam-Vierendeel" truss. Thus, the "beam-Vierendeel" can be analyzed as if it were a true truss with members of proportions and properties as calculated from the known dimensions of the actual beam. As commonly used, the properties of a member are assumed to act about or at its centroidal axis. Lengths of members could be used from center to center of joints. Such a "truss" is shown in Figure 8. The heavy lines indicate the location of the centroidal axis of the members, and therefore, the effective location of the members themselves.

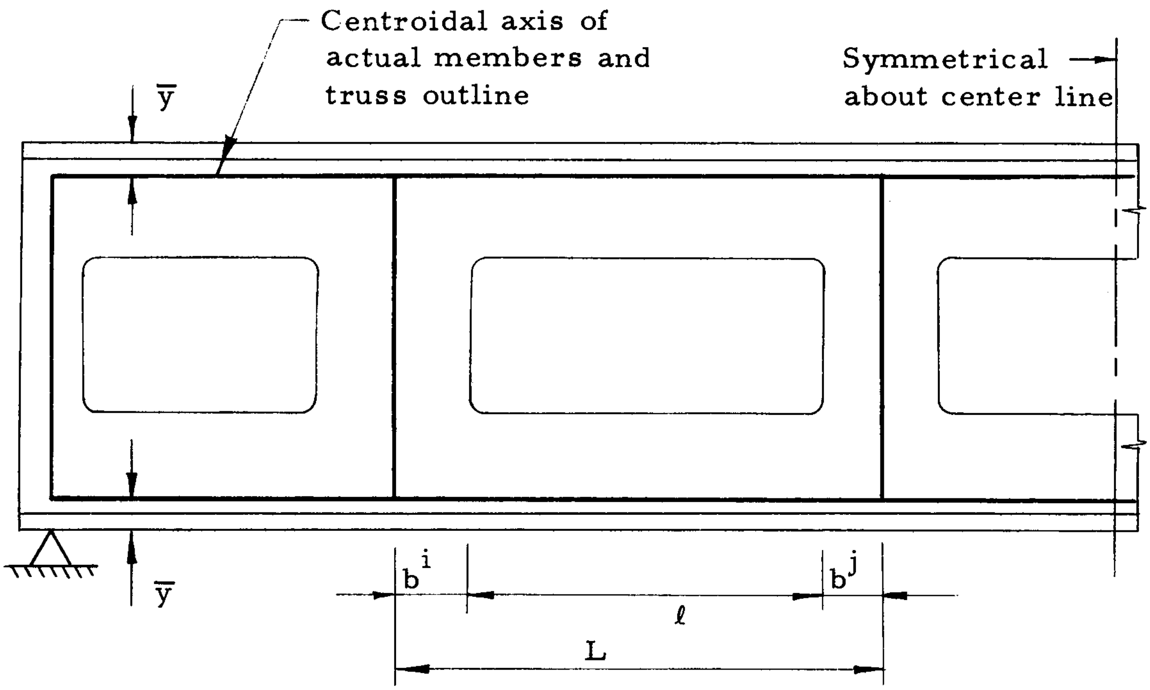

Figure 8. Beam D Reduced to a Truss

However, inspection of the structure shown in Figure 8 with regard to the lengths of members used in this reduced model would show that the large "connections" at the joints are not accounted for in the truss shown. If the stiffness of the "connections" were not included in the analysis, the flexibility of the "beam-Vierendeel" truss would be greatly increased, due to the longer member lengths available for "shear-bending." Although it is recognized by this analysis that the principal bending occurs as "shear-bending" in the tee-sections, it is, in effect, given more emphasis than warranted. The effect of the "connection width" on the length of the tee-sections must be included in the analysis. However, this effect will be included after the general method of solution is presented.

In the development of the displacement method of matrix analysis, the writer assumes that the reader has some knowledge of the principles of the method. This method of analysis is well developed in the literature (6, p. 5; 10, p. 55), and therefore, the principles of the method will not be presented herein. However, the development of the matrix, $[k]$, which relates the member forces (such as bending moment, shear, and axial force) to the internal member displacements (such as rotation, end displacement, and axial shortening), will be shown for the general case, then modified for this particular case. The sign convention adopted is that used by Laursen (10, p. 55) and is shown in Figure 9.

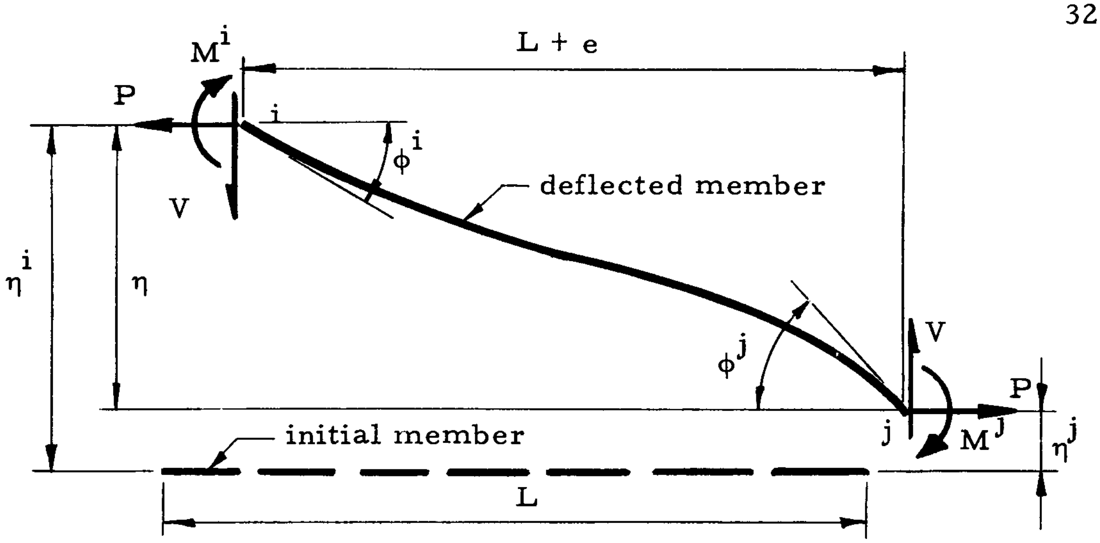

Figure 9. Deflected Member

The small k matrix for a particular member, $[k_i]$, as it is sometimes called, is generally of the form:

$$\begin{bmatrix} M^i \\ M^j \\ V \\ P \end{bmatrix} = \frac{EI}{L} \begin{bmatrix} 4 & 2 & -6/L & 0 \\ 2 & 4 & -6/L & 0 \\ -6/L & -6/L & 12/L^2 & 0 \\ 0 & 0 & 0 & A/I \end{bmatrix} \begin{bmatrix} \phi^i \\ \phi^j \\ \eta \\ e \end{bmatrix} \qquad (3)$$

where

$$[k_i] = \frac{EI}{L} \begin{bmatrix} 4 & 2 & -6/L & 0 \\ 2 & 4 & -6/L & 0 \\ -6/L & -6/L & 12/L^2 & 0 \\ 0 & 0 & 0 & A/I \end{bmatrix} \qquad (4)$$

Terms used in these equations are:

M^i = bending moment at the i end of the member,

M^j = bending moment at the j end of the member,

V = shear in the member,

P = axial force in the member,

E = modulous of elasticity of the material,

L = span length of member,

ϕ^i = rotation at the i end of the member,

ϕ^j = rotation at the j end of the member,

η = deflection at the i end minus the deflection at the j end of the member,

e = axial deformation in the member,

A = cross-sectional area of the member.

An inspection of Equation 3 shows that it could be derived directly from the classical slope deflection equations.

However, Equation 4 is applicable to the general case and must be modified for the solution of the case at hand in which the "connection widths" are to be accounted for. Using slope deflection equations, constants have been derived (8, vol. 107, p. 1000) which can be applied to the small k matrix to compensate for the stiffness of the "connection widths" (7, p. 20). However, in the derivation of the correction constants, the assumption is used that the moment of inertia of the connection width is infinite, provided the joint is symmetrical. That is, members having an equal width frame into the joint on each side of the joint and are perpendicular to the member under consideration.

This restriction is satisfied, in the truss under consideration, by the vertical members (other than the vertical member above the supports) due to the framing-through or continuity through the connections of the tee-sections. When considering the tee-sections, however, the derived constants cannot be applied directly since the vertical members do not continue through the joint in consideration. In this particular case, though, study of the assumptions used in the derivation of the correction constants indicates that a empirical adjustment can be made in the derived quantities. This adjustment is found to be 1/2 and as shown by the experimental results contributes to very good theoretical results (8, vol. 107, p. 1012).

The resulting equation for the small k matrix of a member when the connection width is b^i for the i end and b^j for the j end of the member is:

$$[k_i] = \frac{EI}{L}\begin{bmatrix} 4x_{11} & 2x_{12} & -6x_{13}/\ell & 0 \\ 2x_{21} & 4x_{22} & -6x_{23}/\ell & 0 \\ -6x_{31}/\ell & -6x_{32}/\ell & 12x_{33}/\ell L & 0 \\ 0 & 0 & 0 & A/I \end{bmatrix} \qquad (5)$$

where the correction constants are

$$x_{11} = 1 + 3\,(B^i + B^{i^2})$$

$$x_{12} = x_{21} = 1 + 3\,(B^i + B^j + 2B^iB^j)$$

$$x_{13} = x_{31} = 1 + 2B^i$$

$$x_{22} = 1 + 3\,(B^j + B^{j^2})$$

$$x_{23} = x_{32} = 1 + 2B^j$$

$$x_{33} = 1 + B^i + B^j$$

$$\ell = L - b^i - b^j$$

for which $B^i = \dfrac{b^i C^i}{\ell}$

$$B^j = \frac{b^j C^j}{\ell}$$

The terms C^i and C^j are the adjustment factors at the i and j ends respectively, used to reduce the correction constants for the case in which the constants cannot be applied directly to Equation 4.

Using Equation 5 the small k matrix for all members is calculated, thus forming the small k matrix, $[k]$, for the entire structure. The displacement transformation matrix (10, p. 55) can be formed in the usual manner as with the load matrix.

Since the structure was analyzed by an IBM 1620 digital computer, the program, written in Fortran II, used for the analysis is shown in Appendix B. Note that the input is the displacement transformation matrix, the small k matrix of the structure, and the load matrix. Output is the external member displacements and the internal member forces.

Application to Specimens

The structure used in the analysis was as shown in Figure 8. However, due to the core storage limitations in the available computer, only one-half of the structure was actually analyzed. Since the structure is symmetrical about the center line of the span, the deflections and member forces will also be symmetrical about the center line, provided the loads are symmetrical. Thus, the structure used in this analysis was entirely correct only for type 1 load arrangement.

Reference should again be made to the figures in the Appendix. The actual Vierendeel analysis predicts linear transverse and longitudinal strain distributions as does the approximate Vierendeel analysis. Good agreement is obtained near the center of the holes with reference to both the strain distributions and the inflection point location. However, near the edges of the holes, predictions are not as good as by the approximate method. This disagreement is due in part to the inexact analysis at the joint.

The deflections calculated by this method, as shown in Table 1, are in very good agreement with the experimental deflections. As previously noted, the calculated deflections for load types 2 and 3, are not precise because the loads are not symmetrical. However, inspection of the tabulated deflections indicate that for load types 2 and 3 reasonable approximations are still obtained. The deflections are also tabulated for the structure analyzed without consideration of the "connection-widths." These values are at all times conservative.

Part 6

THEORY OF ELASTICITY SOLUTION

The Applied Research Laboratory (2, p. 3) recently developed and presented a method whereby the theory of elasticity is applied to the analysis of a beam with web holes. Due to the complexities of the solution, the development of the method is not included herein, but rather, a discussion of the results obtained by the analysis.

The analysis is based on the assumption that stress functions can be determined for the stresses at the boundaries of the hole. These stress functions are to be composed of two parts: (1) stress functions for the beam without a hole and (2) stress functions which when combined with functions of (1) satisfy the known boundary conditions at the hole edges. However, no boundary conditions are included for the transverse boundaries of the beam. This may, therefore, render the entire analysis inapplicable for beams with large vertical hole dimensions.

Solution by the theory of elasticity method is very complex and virtually requires a computer solution. Results from such an analysis are in excellent agreement with experimental stresses near circular holes (3, p. 12). However, for rectangular holes, agreement is, in general, good only at the stress concentrations at the fillets. Octahedral stresses predicted by this method are in better agreement with the experimental stresses near the hole boundary rather than vertically away from the hole.

Due to the complexities of this method of analysis, no comparisons with other methods, or with the experimental results are presented in this thesis. Applications of this method are being studied further.

CONCLUSIONS AND RECOMMENDATIONS

For the particular beam specimens tested, correlation between the strain distributions from the experimental studies to the predicted strain distributions by the methods presented herein is good. Near the center of the hole accuracy of prediction by both methods is the greatest. Thus, it may be concluded that the specimens tested behaved as an actual Vierendeel truss. However, stress concentrations near the hole corners cause non-linear strain distributions which cannot be precisely determined by the methods of the Vierendeel analysis. To determine the magnitudes of these corner concentrations, the theory of elasticity analysis must be used. Due to the complexities of this method of analysis, design tables or charts should be accumulated.

With adjustments made in the actual Vierendeel analysis for the stiffness of the "connection widths," accurate predictions of the beam deflections are determined. On a large computer the entire structure, including deflections, could be analyzed in a matter of minutes by the actual Vierendeel method of analysis.

Failure of the beam specimens was by web instability over the supports. However, at the relatively high loads encountered near failure, the tee-sections were not found to be unstable, nor did the flange strains go beyond the elastic range of the material. The largest experimental strains in the tee-sections were, in all cases, located near the hole corners.

Future tests should be conducted on similar test specimens with the upper flange secured to prevent lateral movement, or with web plate stiffners over the support. More work should be done to determine the effect of the closeness of adjacent holes on the strain distributions near the hole corners. Experimental work is also recommended to determine the effect of the corner radius on the stress concentrations near the corners. Continued experimental and analytical studies should be made to determine the stiffness adjustment factors, which should be applied to unsymmetrical "joints" in the actual Vierendeel analysis.

BIBLIOGRAPHY

1. Baes, Louis. Rigid frames without diagonals (The Vierendeel truss). Transitions of the American Society of Civil Engineers 107: 1215-1228. 1942.

2. Bower, John E. Elastic stresses around holes in the web of wide-flange beams. Monroeville, Pennsylvania, United States Steel Corporation, November 17, 1964. 29 p. (Applied Research Laboratory Report 57. 019-400(6))

3. ________________. Experimental elastic stresses in wide-flange beams with web holes. Monroeville, Pennsylvania, United States Steel Corporation, January 31, 1966. 26 p. (Applied Research Laboratory Report 57. 019-400(10))

4. ________________. Suggestions for research - holes in beam webs. Joint ASCE-AASHO Task Committee on Flexural Members. Subcommittee 5-Castellated Beams. Committee Correspondence, Monroeville, Pennsylvania, January 19, 1966. 5 p.

5. Cato, Stuart Leslie. Web buckling failure of built-up girders with rectangular holes. Master's thesis. Corvallis, Oregon State University, 1964. 37 numb leaves.

6. Clough, Ray W. Use of modern computers in structural analysis. Proceedings of the American Society of Civil Engineers: Journal of the structural division. Vol. 84 no. ST3. Paper no. 1636. 20 p.

7. Grant, Joseph. Matrix analysis of structures with semi-rigid connections. Master's thesis. Corvallis, Oregon State University, 1965. 34 numb. leaves.

8. Johnston, Bruce G. and Edward H. Mount. Analysis of building frames with semi-rigid connections. Transactions of the American Society of Civil Engineers 107: 993-1018. 1943.

9. Landers, William. Web stresses in Vierendeel girders. Unpublished research. Corvallis, Oregon State University Engineering Experiment Station, 1965.

10. Laursen, Harold I. Matrix analysis of structures. New York, McGraw Hill, 1966. 159 p.

11. Lee, George Hamor. An introduction to experimental stress analysis. New York, John Wiley & Sons, 1950. 319 p.

12. Roark, Raymond J. Formulas for stress and strain. 3d ed. New York, McGraw-Hill, 1954. 381 p.

13. Roik, Stephen A. and William Almdal. An investigation of the effects of reinforcing on a rectangular hole in the web of a steel beam. Bachelor's thesis. Winnipeg, University of Manitoba, 1963. 30 numb leaves.

14. Savin, G. N. Stress concentrations around holes. London, Pergamon Press, 1961. 427 p.

15. Segner, Edmund P., Jr. Reinforcement requirements for girder web openings. Proceedings of the American Society of Civil Engineers: Journal of the structural division. Vol. 90 no. ST3. p. 147-164. 1964.

16. ________________. An investigation of the requirements for reinforcement around large rectangular openings in the webs of wide-flange beams subject to bending moment and shear. College Station, Texas A and M Engineering Experiment Station No. E-81-62, 1963. 30 p.

17. Serpanos, James E. Stiffness matrix analysis of structures by electronic digital computer. Master's thesis. Corvallis, Oregon State University, 1963. 85 p.

APPENDICES

APPENDIX A

Tables and Graphs

Table A. 1. Rosette stresses in kips per square inch

Beam	Load Type	Gage No.	Measured Stresses (from experimental strains) Horizontal	Vertical	Principal Stresses (from experimental strains) Maximum	Minimum	Max. Shear Stress	Direction of Principal Stress, Degrees
C	1	R-1	17.59	3.17	22.26	0.25	11.19	23.5
		R-2	13.42	-1.19	- 0.88	-14.96	7.15	12.8
		R-3	4.58	1.65	7.91	- 1.16	4.61	35.1
	2	R-1	15.68	2.75	19.41	0.58	9.57	22.2
		R-2	-20.03	-2.44	- 0.81	-23.54	11.55	18.2
		R-3	11.39	2.80	15.35	0.03	7.78	27.1
	3	R-1	10.05	1.90	12.49	0.47	6.11	22.6
		R-2	-12.82	-1.29	- 0.37	-14.94	7.40	17.3
		R-3	7.42	1.92	10.02	0.10	5.04	27.4
D	1	R-1	15.37	1.65	18.68	- 0.22	9.61	20.5
		R-2	-12.51	0.37	1.69	-14.85	8.41	18.0
		R-3	4.49	1.20	7.06	- 0.88	4.04	32.3
	2	R-1	12.31	1.10	15.08	- 0.53	7.94	20.9
		R-2	-19.33	-0.20	2.43	-23.42	13.14	19.5
		R-3		(defective)				
	3	R-1	7.72	0.94	9.60	- 0.20	4.98	22.0
		R-2	-12.12	0.20	1.49	-14.42	8.09	18.2
		R-3		(defective)				

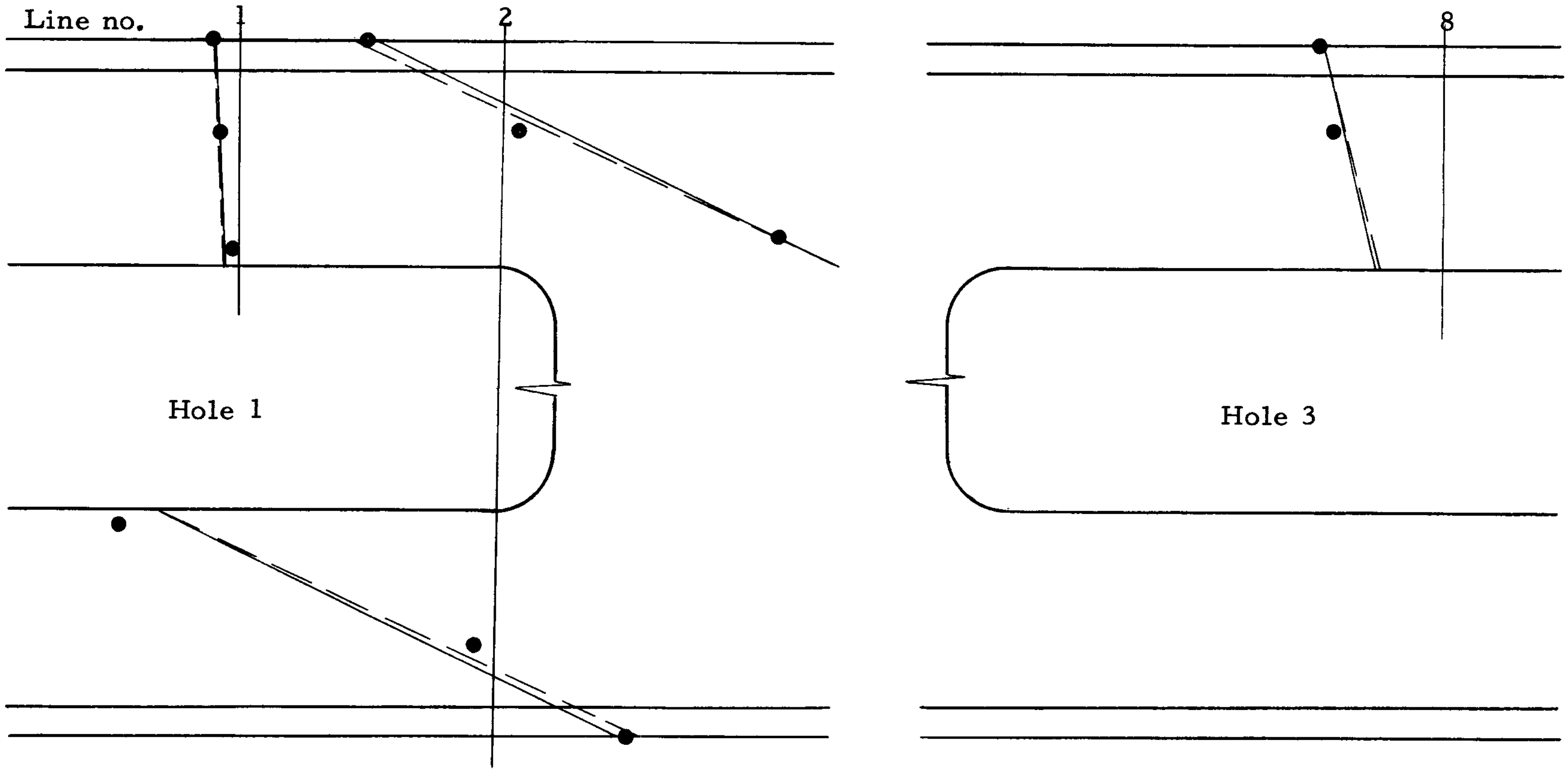

— — — Approximate Vierendeel distribution
——— Actual Vierendeel distribution   Horizontal scale: 1 in. = 400×10^{-6} in./in.
● Experimental strains
Note: Left of transverse line indicates a compressive strain and right of transverse line indicates a tensile strain.

Figure A. 1. Transverse strain distribution for Lines 1, 2, and 8 on Beam C, load type 1.

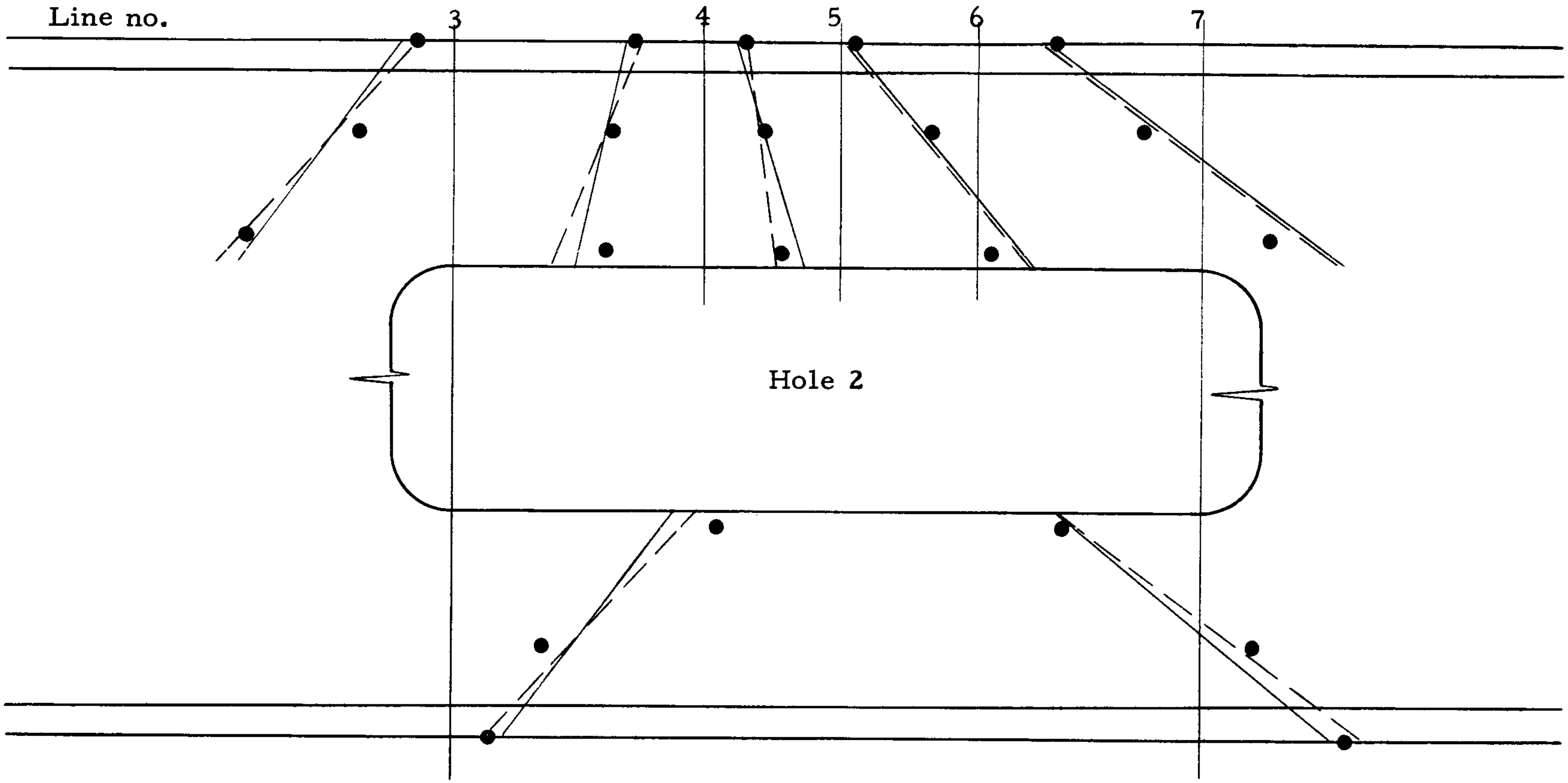

— — — Approximate Vierendeel distribution

——— Actual Vierendeel distribution

● Experimental strains

Horizontal Scale: 1 in. = 400×10^{-6} in/in.

Note: Left of transverse line indicates a compressive strain and right of transverse line indicates a tensile strain.

Figure A. 2. Transverse strain distribution at Hole 2 for Beam C, load type 1.

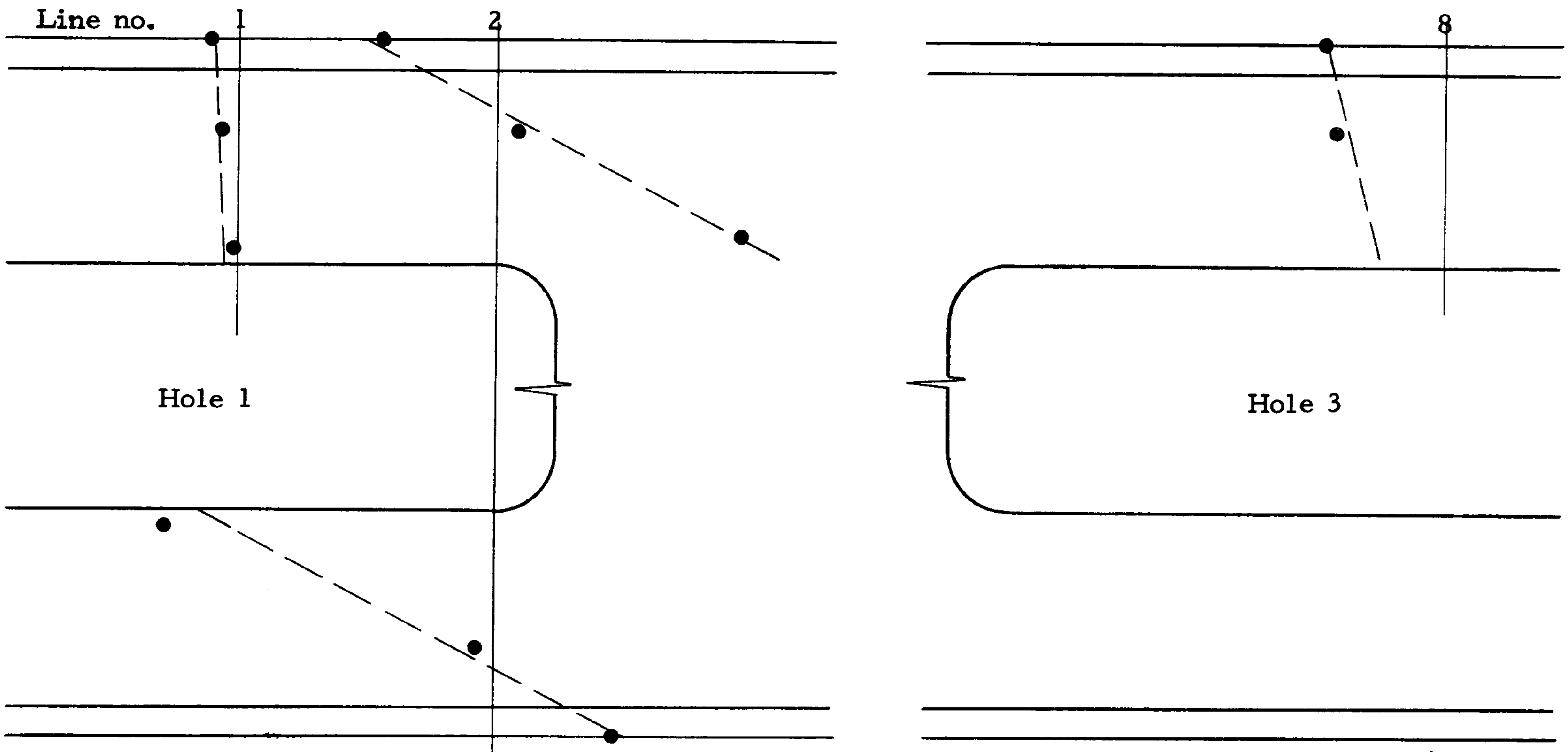

— — — Approximate Vierendeel distribution

● Experimental strains

Horizontal Scale: 1 in. = 400×10^{-6} in./in.

Note: Left of transverse line indicates a compressive strain and right of transverse line indicates a tensile strain

Figure A. 3. Transverse strain distribution for Lines 1, 2, and 8 on Beam C, load type 2.

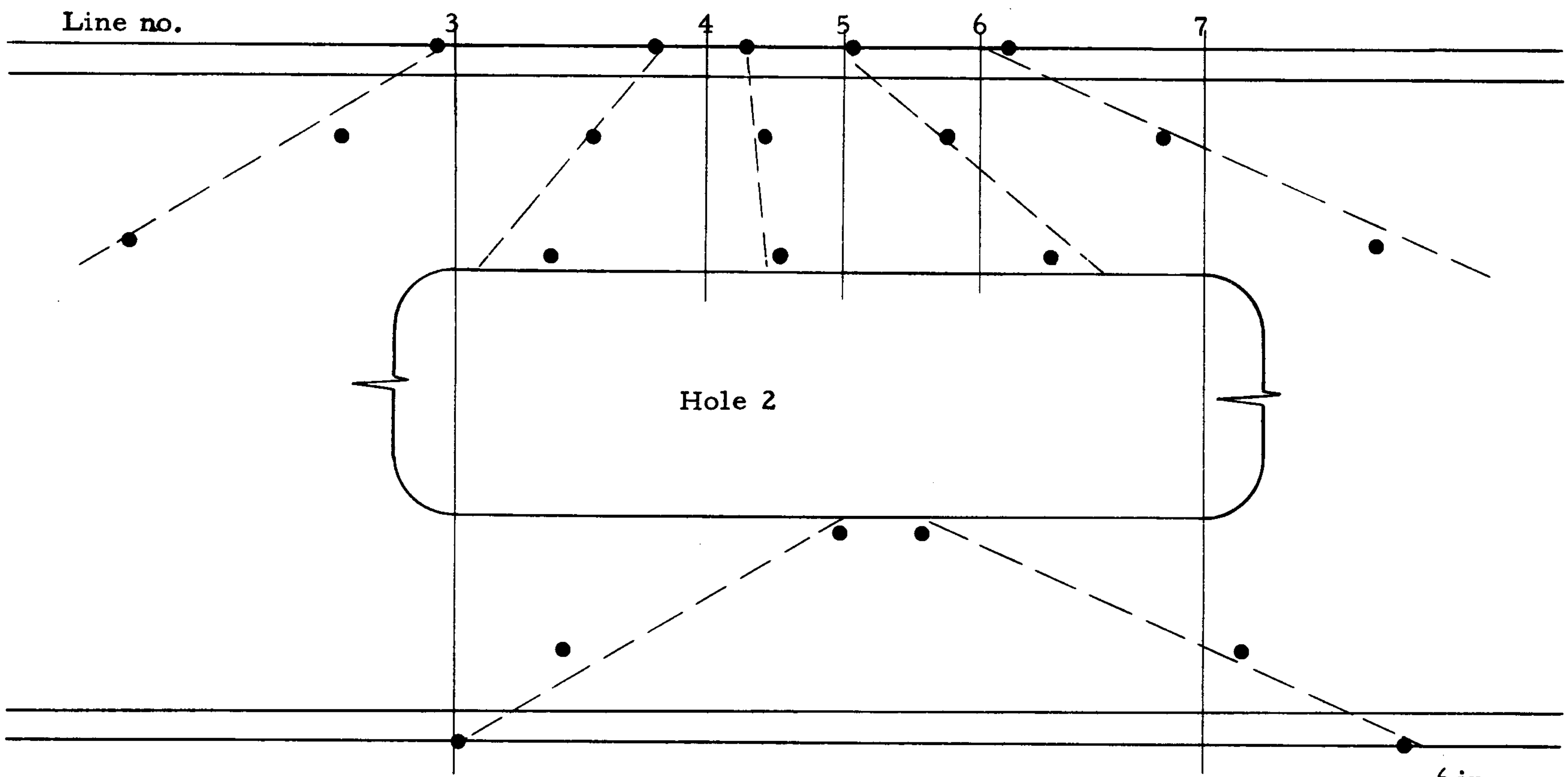

— — —Approximate Vierendeel distribution Horizontal Scale: 1 in = 400 x 10^{-6} in./in.

● Experimental strains

Note: Left of transverse line indicates a compressive strain and right of transverse line indicates a tensile strain

Figure A.4. Transverse strain distribution at Hole 2 for Beam C, load type 2.

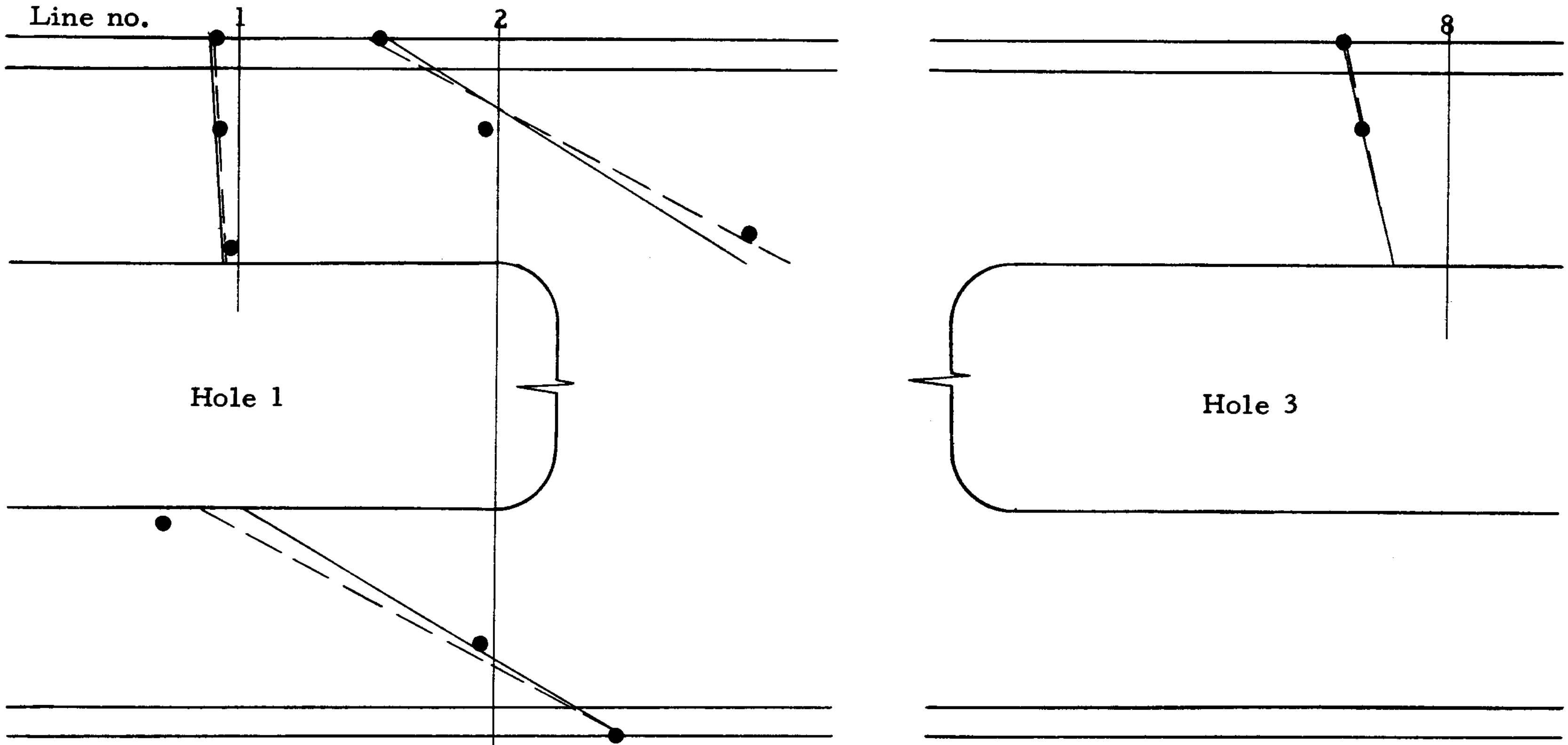

— — — Approximate Vierendeel distribution
——— Actual Vierendeel distribution
● Experimental strains

Horizontal Scale: 1 in. = 400×10^{-6} in./in.

Note: Left of transverse line indicates a compressive strain and right of transverse line indicates a tensile strain.

Figure A. 5. Transverse strain distribution for Lines 1, 2, and 8 on Beam D, load type 1.

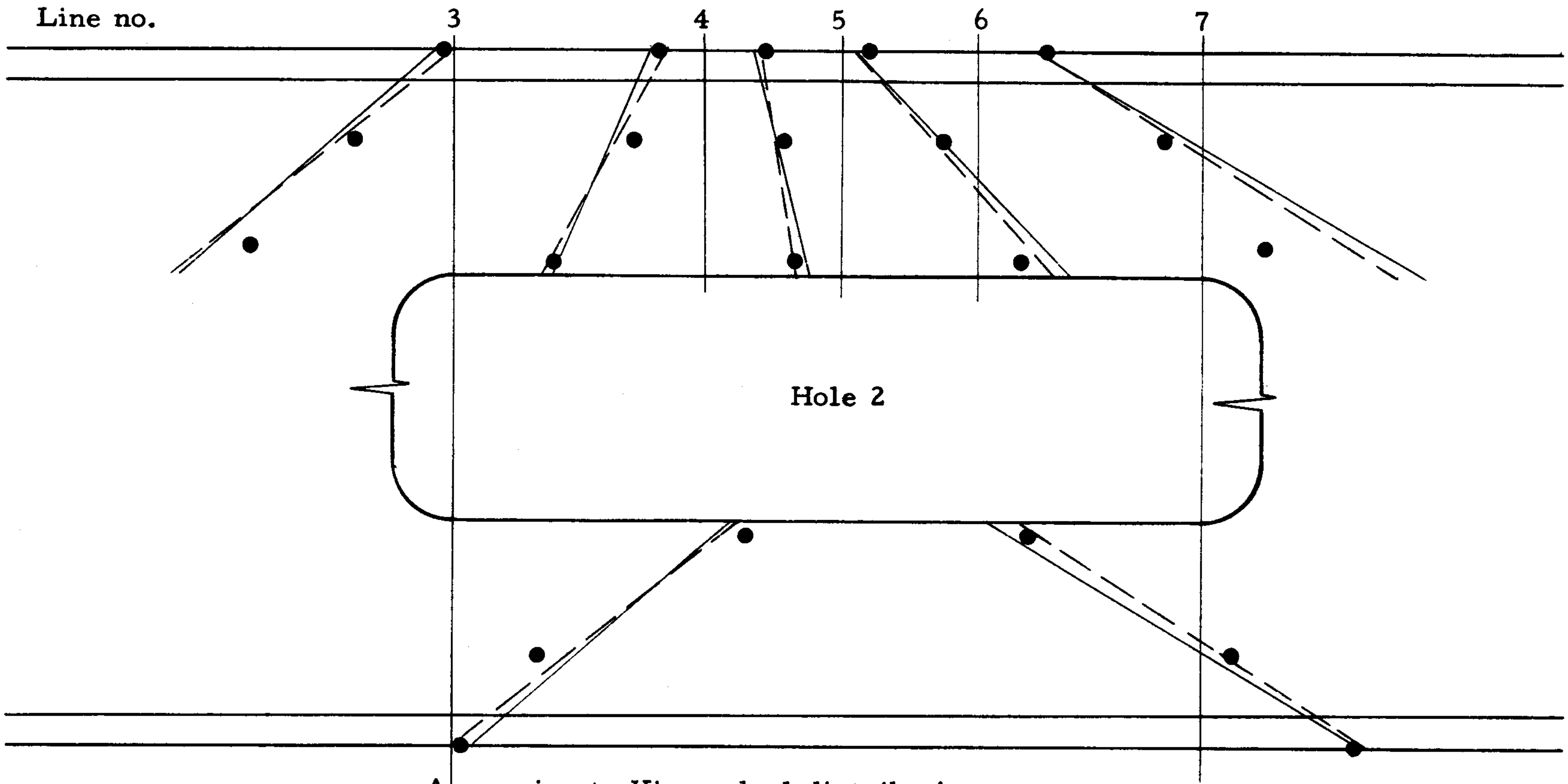

— — — Approximate Vierendeel distribution

——— Actual Vierendeel distribution   Horizontal Scale: 1 in. $= 400 \times 10^{-6}$ in./in.

● Experimental strains

Note: Left of transverse line indicates a compressive strain and right of transverse line indicates a tensile strain

Figure A. 6. Transverse strain distribution at Hole 2 for Beam D, load type 1.

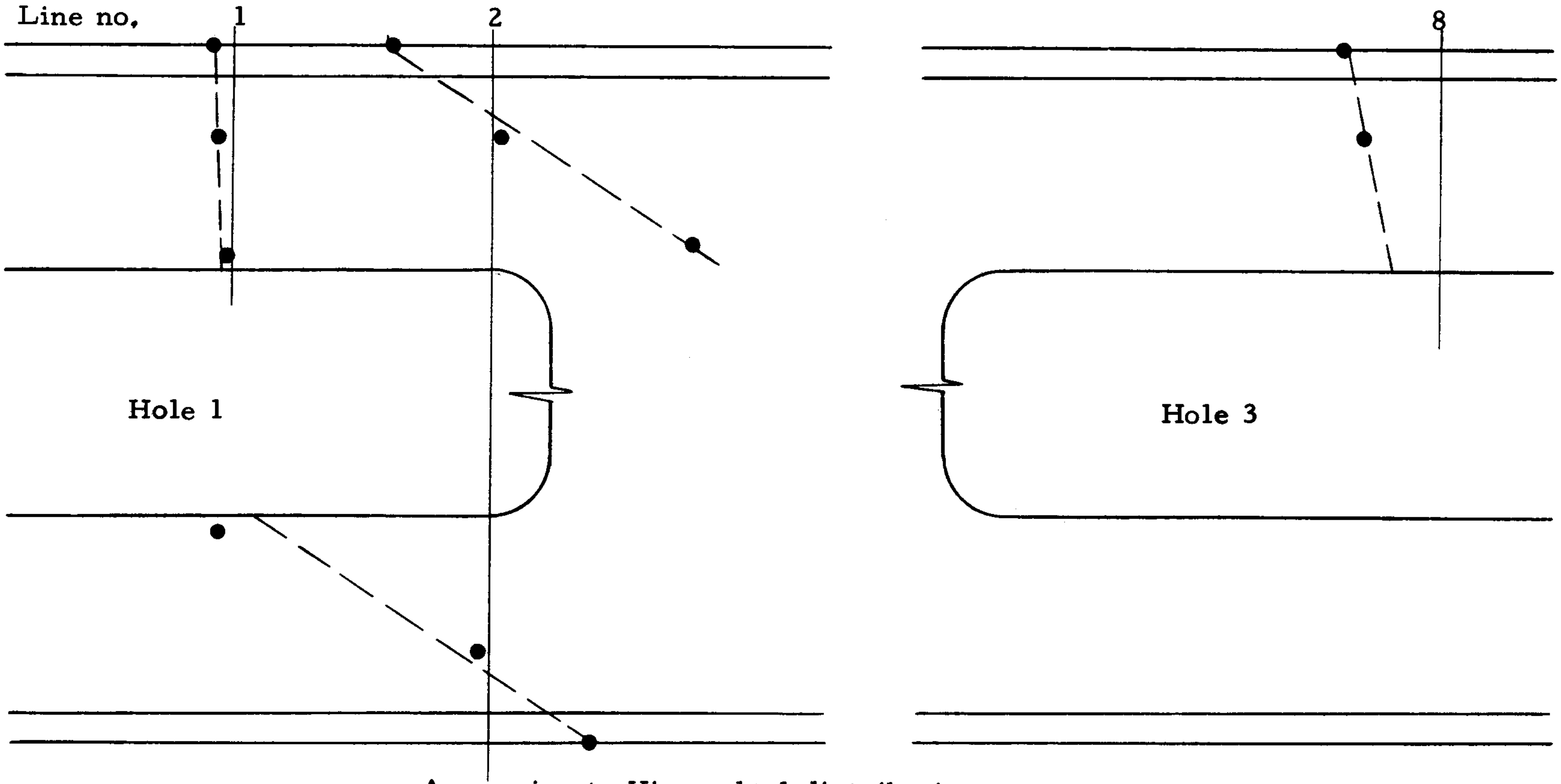

— — — Approximate Vierendeel distribution

● Experimental strains

Horizontal Scale: 1 in. = 400×100^{-6} in./in.

Note: Left of transverse line indicates a compressive strain and right of transverse line indicates a tensile strain

Figure A. 7. Transverse strain distribution for Lines 1, 2, and 8 on Beam D, load type 2.

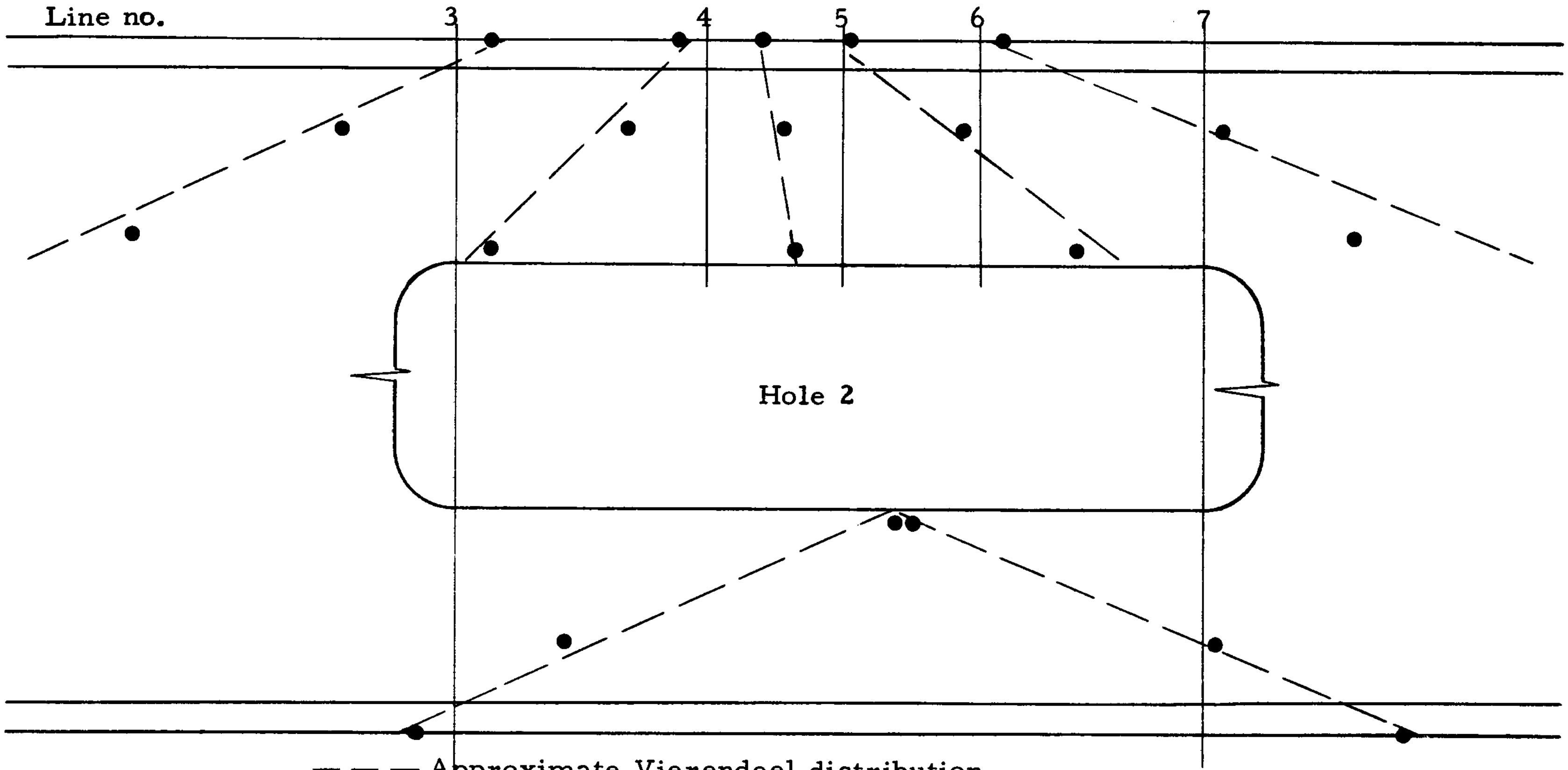

— — — Approximate Vierendeel distribution

● Experimental strains

Horizontal Scale: 1 in. = 400×10^{-6} in./in.

Note: Left of transverse line indicates a compressive strain and right of transverse line indicates a tensile strain

Figure A. 8. Transverse strain distribution at Hole 2 for Beam D, load type 2.

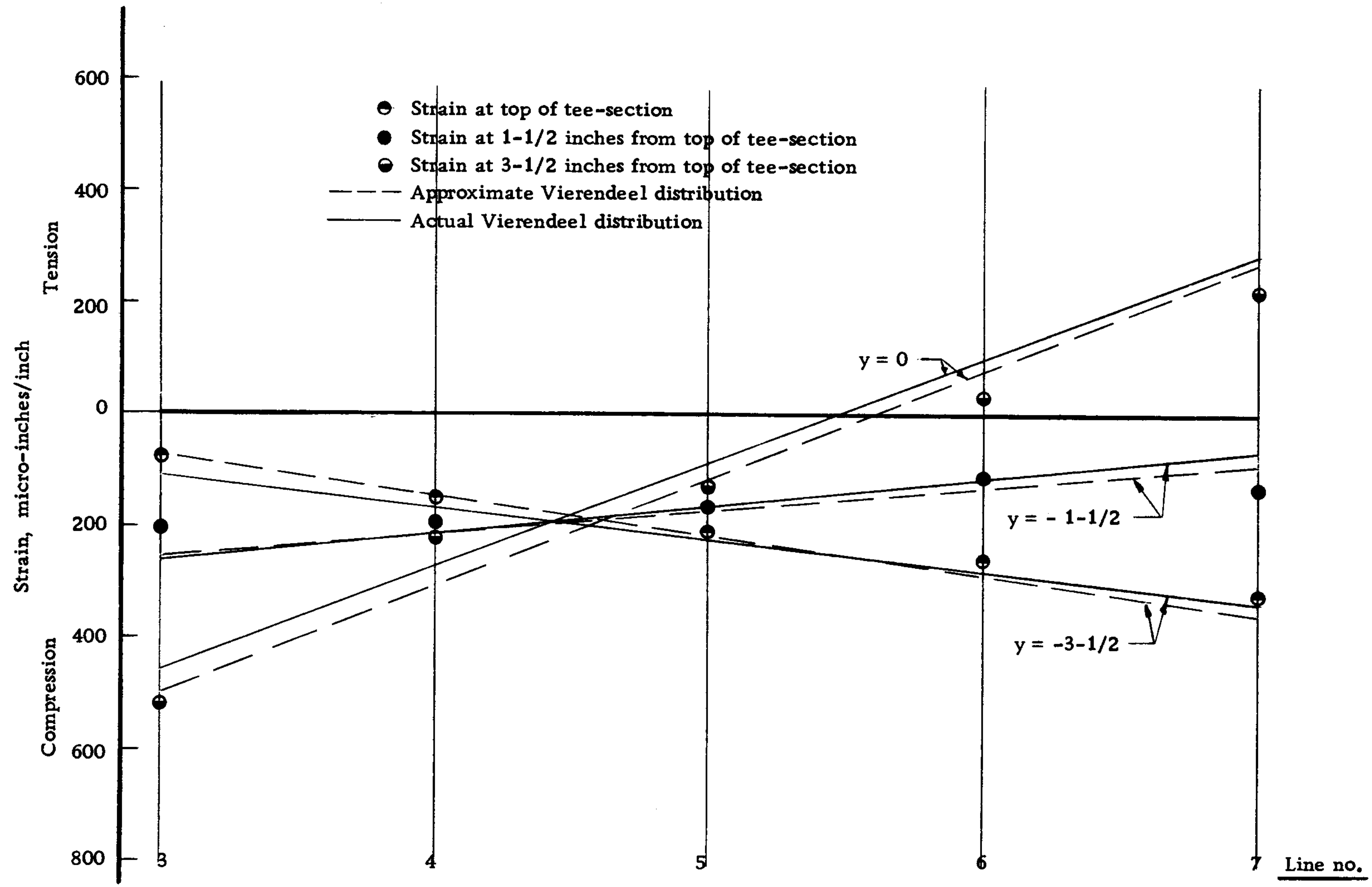

Figure A. 9. Longitudinal strain distribution along upper tee-section of Hole 2 for Beam C, load type 1.

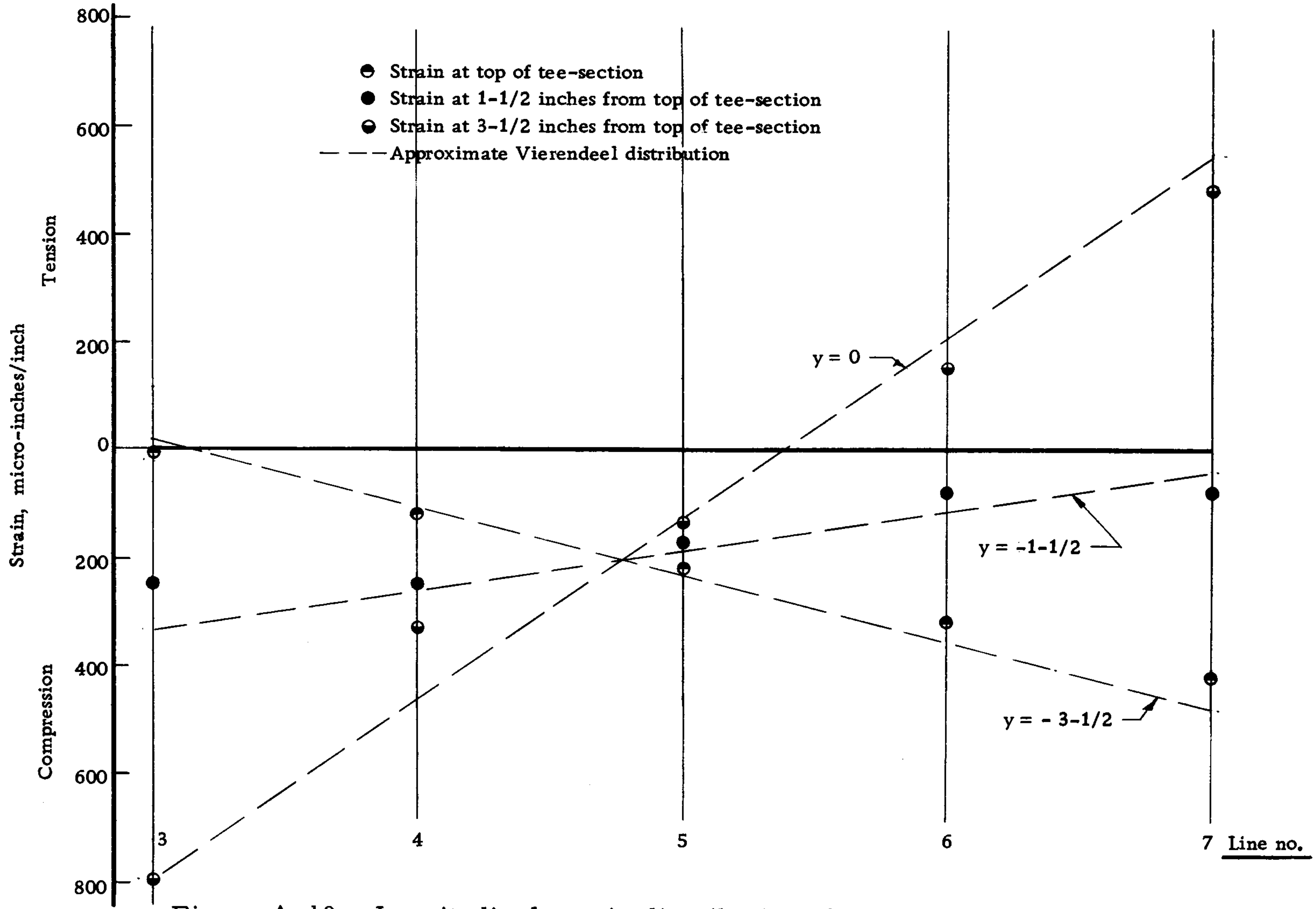

Figure A. 10. Longitudinal strain distribution along upper tee-section of Hole 2 for Beam C, load type 2.

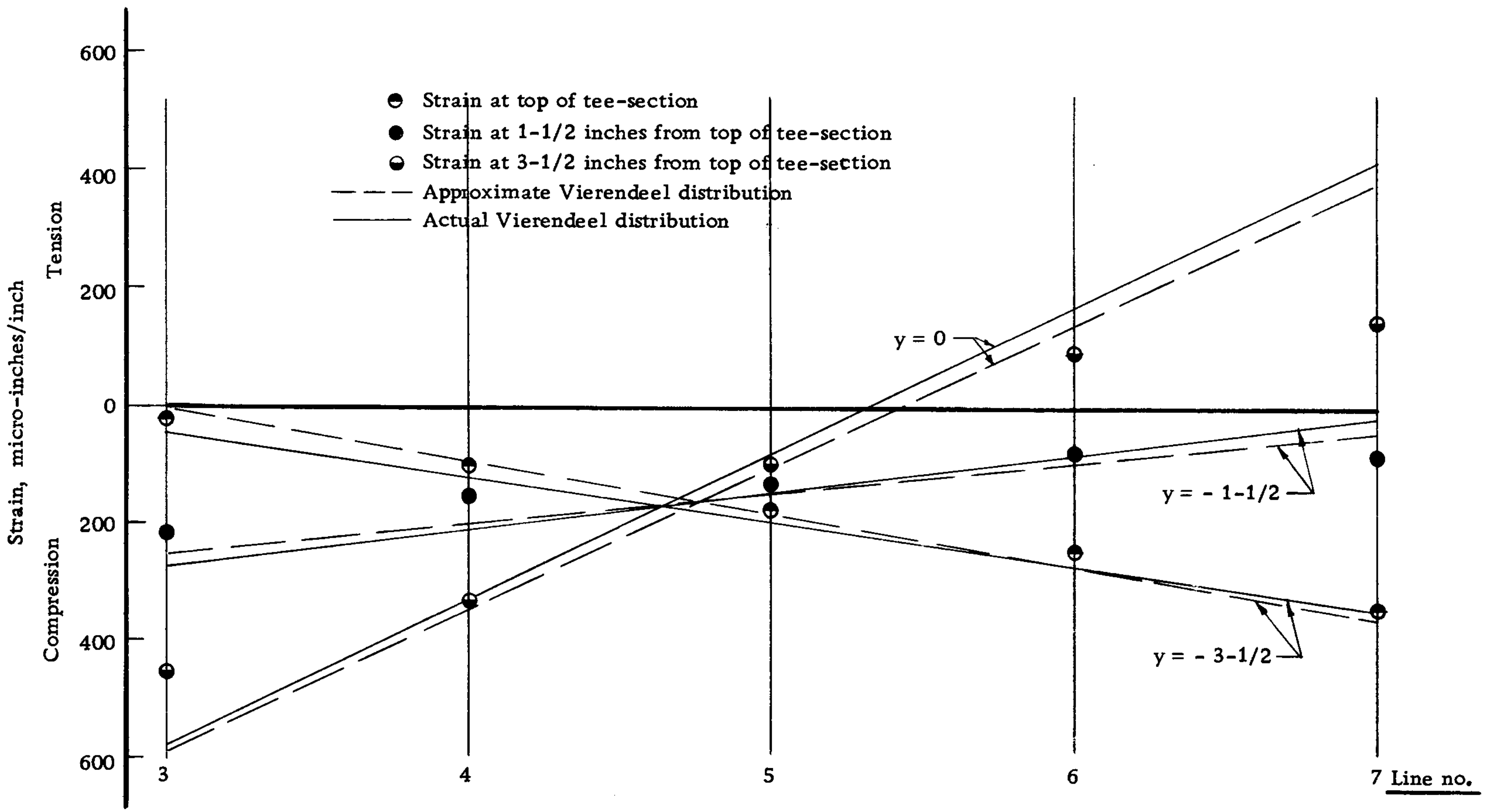

Figure A. 11. Longitudinal strain distribution along upper tee-section of Hole 2 for Beam D, load type 1.

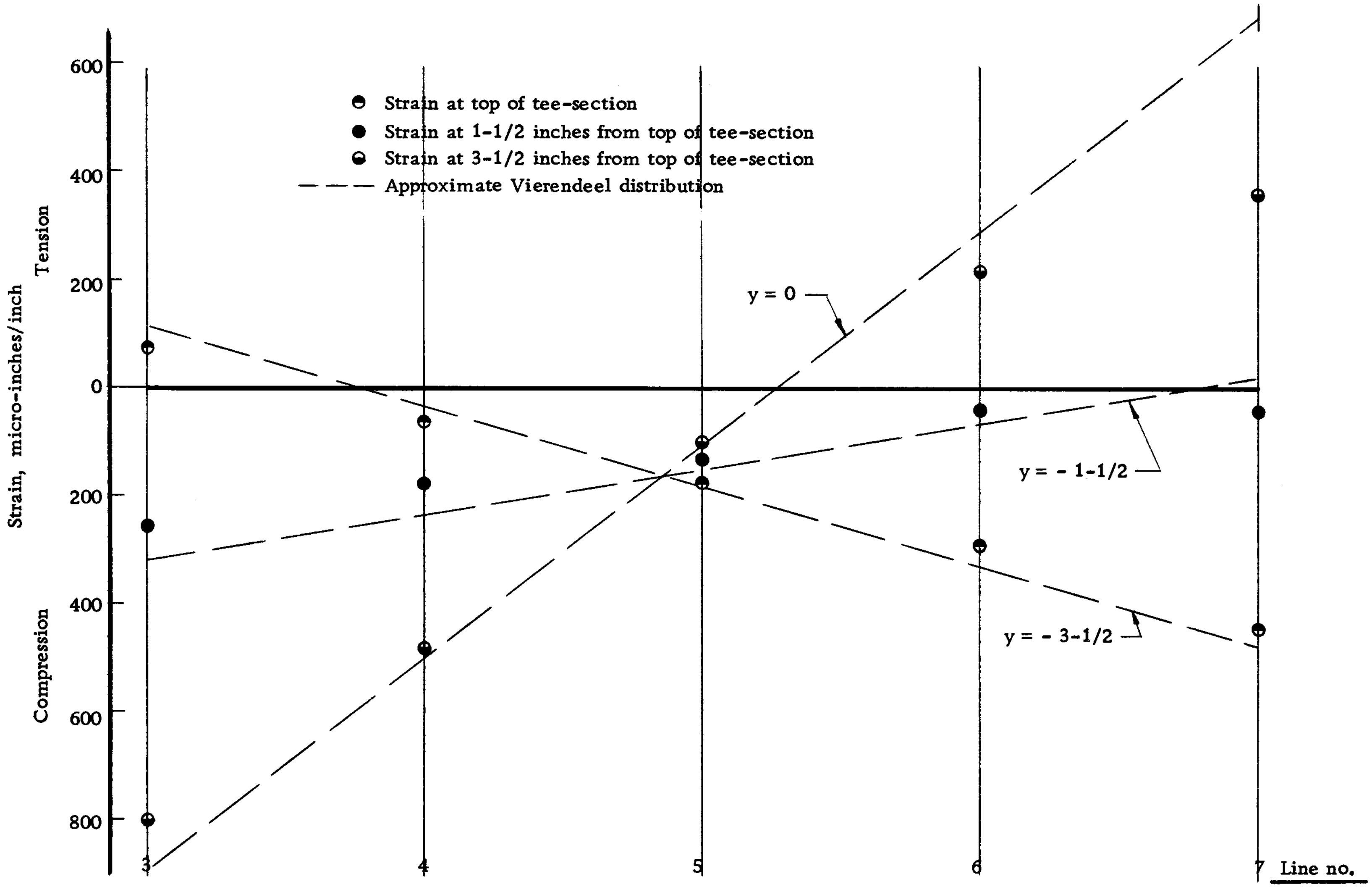

Figure A. 12. Longitudinal strain distribution along upper tee-section of Hole 2 for Beam D, load type 2.

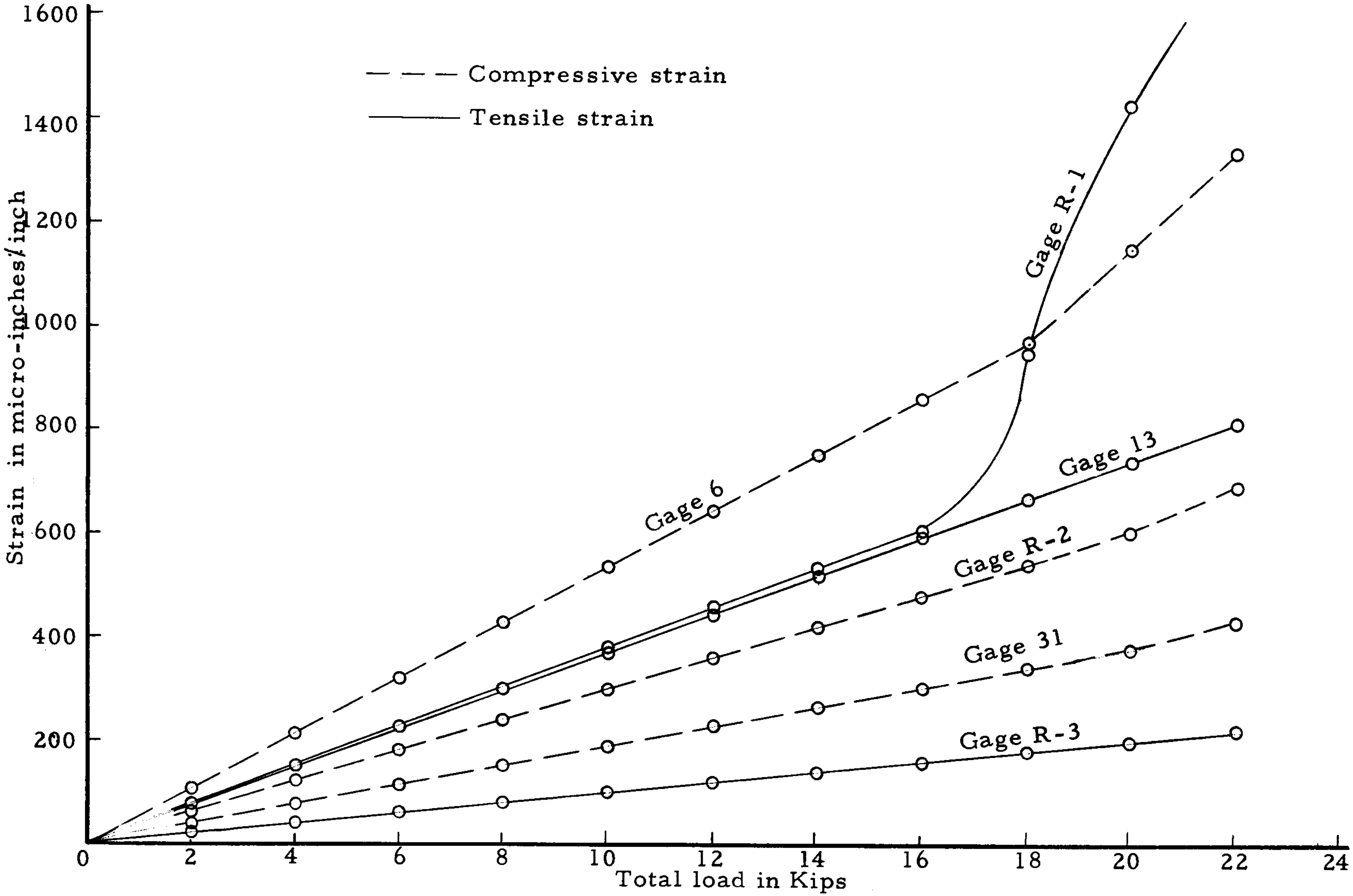

Figure A. 13. Ultimate load test curves for Beam C.

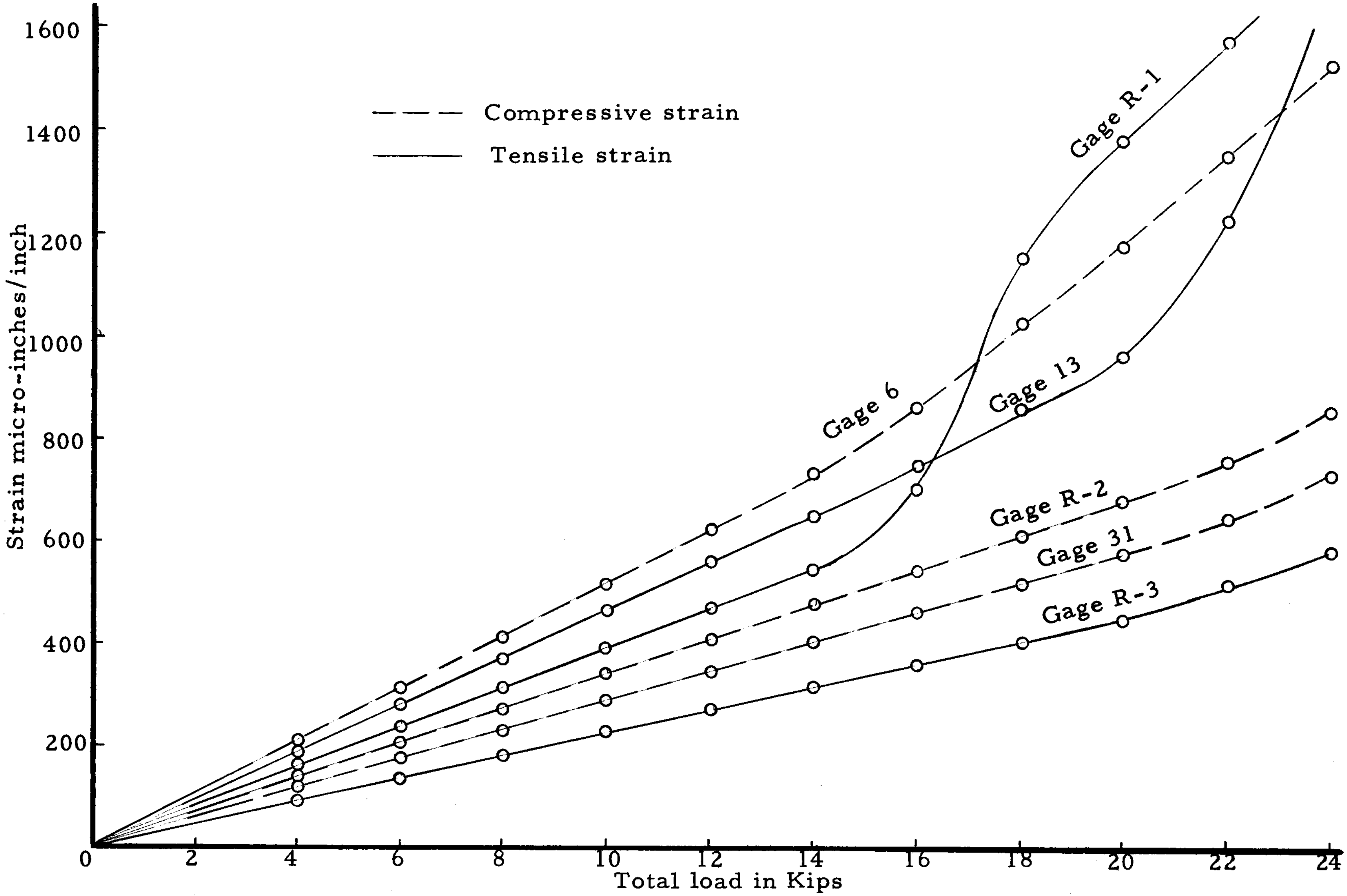

Figure A. 14. Ultimate load test curves for Beam D.

APPENDIX B

Computer Programs

Matrix Analysis of Indeterminate Structure by Displacement Method

```
      DIMENSION A(36, 18), SMK(36, 4) , BGK(18, 18), F(18, 36), Q(36), D(18)
      COMMON BGK
30    READ 18, M, N, JOBNO , KSIZE
      PUNCH 27, JOBNO
61    DO 62 I = 1, M
      DO 62 J = 1, N
62    A(I, J) = 0.0
63    READ 41, I, J, AB, III
      A(I, J) = AB
      IF (III) 65, 63, 65
65    DO 17 I = 1, M
17    READ 42, (SMK(I, J), J = 1, KSIZE)
      DO 1 I = 1, N
      DO 1 K = 1, M, KSIZE
      DO 1 J = 1, KSIZE
      KMAX = K + KSIZE - 1
      KXXX = K + J - 1
      F(I, KXXX) = 0.0
      DO 1 L = K, KMAX
 1    F(I, KXXX) = F(I, KXXX) + A( L, I) * SMK(L, J)
      DO 2  I = 1, N
      DO 2  J = 1, N
      BGK(I, J) = 0.0
      DO 2  L = 1, M
 2    BGK(I, J) = BGK(I,J) + F(I, L)*A(L, J)
      CALL MATINV(BGK, N)
15    READ 21, (Q(I), I = 1, N)
      PUNCH 31
      PUNCH  20, (Q(I),  I = 1, N)
      DO 5 I = 1, N
      D(I) = 0.0
      DO 5 L = 1, N
 5    D(I) = D(I) + BGK(I, L)*Q(L)
      DO 7 I = 1, M
      Q(I) = 0.0
      DO 7  L=1, N
 7    Q(I) = Q(I) + F(L, I) * D(L)
      PUNCH 26
      IF(M-N)8, 11, 11
 8    DO 9 I = 1, M
 9    PUNCH 22, I, D(I), Q(I)
      L = M + 1
      DO 10 I = L, N
10    PUNCH 22, I, D(I)
      GO TO 14
11    DO 12  I = 1, N
12    PUNCH 22, I, D(I), Q(I)
      L = N + 1
      DO 13 I = L, M
```

```
13    PUNCH 23, I, Q(I)
14    PAUSE
      IF (SENSE SWITCH 1)30, 15
18    FORMAT (4I2)
20    FORMAT (7F11.6)
21    FORMAT (9F8.2)
22    FORMAT (I3, 2X, E14.5, 2X, E14.5)
23    FORMAT (I3, 18X, E14.5)
26    FORMAT(//35HNUM DEFLECTION*EI/L  MEMBER FORCES/)
27    FORMAT (5HJOBNO, I5//)
31    FORMAT (//14HLOADING MATRIX/)
41    FORMAT (2I2, F8.6, I2)
42    FORMAT (6F12.6)
      END
```

MATRIX INVERSION

```
      SUBROUTINE MATINV(A, N)
      DIMENSION A(18, 18)
      COMMON A
      DO 5 K = 1, N
      COM = A(K, K)
      A(K, K) = 1.0
      DO 2 J = 1, N
2     A(K, J) = A(K, J) / COM
      DO 5 I = 1, N
      IF (I-K) 3, 5, 3
3     COM = A(I, K)
      A(I, K) = 0.0
      DO 4 J = 1, N
4     A(I, J) = A(I, J) - COM * A(K, J)
5     CONTINUE
      RETURN
      END
```